



# Technical Report HALCYON

Team 01 Technical Report to the 2023 EuRoC



Aerospace Team Graz (ASTG)  
Graz University of Technology, Austria

Graz, October 2, 2023

Contact: [s.liebhart@astg.at](mailto:s.liebhart@astg.at)



## Abstract

Project HALCYON is the first hybrid rocket built by the Aerospace Team Graz (ASTG), competing in the H3 (SRAD hybrid 3 km) category at the European Rocketry Challenge (EuRoC) 2023. After the successful participation in the last two installments of the challenge, HALCYON aims to maintain or surpass the high standards that have been established in those years. By going from solid to hybrid propulsion, the team wants to advance its knowledge and abilities in the field of rocketry, setting up the stage for even more sophisticated projects in the future.

The launch vehicle has an overall length of 3.57 m with an outer diameter of 152 mm and a launch mass of 32 kg. Housed inside the nose cone are the official tracking computer and the payload of three CubeSats, two of which were built by high school students in an effort to promote the next generation of rocketry enthusiasts. Additionally, one CubeSat with a stabilized camera was developed as part of a Bachelor thesis. Continuing down is the dual deployment recovery system with main- and drogue parachute, and telemetry patch antennas attached to the outer hull. Right below the recovery section, the main electronics bay is mounted. It houses the self-developed flight computer, the redundant recovery electronics, as well as a second telemetry antenna. Situated further down is the pressurizing system for the rocket's propulsion. Utilizing nitrogen, it ensures near-constant pressure in the 5.5 L nitrous oxide tank during the boost phase. The two tank bulkheads are equipped with integrated fluid ports, sensor mounts, and structural attachment points. Mounted to the lower bulkhead are the servo-actuated main valve, several safety devices, and the aluminium 3D-printed thrust structure. Last in line comes the combustion chamber, housing the paraffin fuel, capped off by the swirl injector at the top and the graphite nozzle at the bottom. Enclosing all systems is the airframe, consisting of a series of carbon fibre- and glass fibre-reinforced plastic tubes. Its most recognizable component are the four fins made in lightweight sandwich construction. Positioned between two fins is the downward-facing tail camera, which provides some of the best camera views during a flight.

Due to the nature of the hybrid propulsion system, a major effort was put into developing and building the necessary ground support equipment: The filling station, which prepares the liquid  $N_2O$  and fills it into the rocket, together with the high-pressure  $N_2$ , and the telemetry ground station which provides the necessary data readouts and actuator controls at a safe distance.

For a complex system like HALCYON to work reliably, an extensive testing campaign is required. After various individual system tests, everything culminated in a flight test in mid-August 2023. With the successful launch and recovery of the rocket already achieved once, we are confident to repeat it at EuRoC in Portugal.



# Contents

<b>1</b>	<b>Introduction</b>	<b>7</b>
1.1	Team Introduction and Overview . . . . .	7
1.2	Team Structure . . . . .	8
1.3	Partners and Supporters . . . . .	9
1.4	Project Goals . . . . .	9
1.5	Mission Objectives . . . . .	9
<b>2</b>	<b>Launch Vehicle System Architecture</b>	<b>11</b>
2.1	Overview . . . . .	11
2.2	Propulsion Subsystem . . . . .	12
2.2.1	Fluid System . . . . .	13
2.2.2	Combustion Chamber . . . . .	15
2.2.3	Ignitor . . . . .	17
2.2.4	Propulsion Testing . . . . .	18
2.3	Aerostructure Subsystem . . . . .	20
2.3.1	Shell . . . . .	20
2.3.2	Aerodynamics . . . . .	21
2.3.3	Payload Structure . . . . .	22
2.3.4	Coupling Tube and Pressure Chamber . . . . .	23
2.3.5	Radax . . . . .	23
2.3.6	Oxidizer Tank . . . . .	24
2.3.7	Thrust Structure and Motor Retention . . . . .	25
2.3.8	Retractable Railbutton . . . . .	26
2.4	Recovery Subsystem . . . . .	27
2.4.1	First Deployment . . . . .	27
2.4.2	Second Deployment . . . . .	29
2.4.3	Parachutes and Lines . . . . .	30
2.5	Flight Computer Subsystem . . . . .	35
2.5.1	Recovery Electronics . . . . .	35
2.5.2	Sensor and Control Nodes CANary . . . . .	36
2.5.3	Power Management . . . . .	36
2.5.4	Electronics Mount . . . . .	37
2.5.5	Mainboard and Backplane . . . . .	38
2.5.6	State Diagram and Software . . . . .	38
2.6	Telemetry Subsystem . . . . .	41
2.6.1	Software . . . . .	41
2.6.2	Visualization . . . . .	42
2.6.3	Hardware . . . . .	42
2.6.4	Antennas . . . . .	44
2.7	Payload Subsystem . . . . .	45
2.7.1	CubeSat Colibri . . . . .	45
2.7.2	CubeSat PATHOA . . . . .	45
2.7.3	HPD's CubeSat . . . . .	45

<b>3</b>	<b>Ground Support Equipment System Architecture</b>	<b>47</b>
3.1	Filling Station . . . . .	47
3.1.1	Fluid Architecture . . . . .	47
3.1.2	Electronics Architecture . . . . .	48
3.1.3	Safety Precautions . . . . .	48
3.1.4	State Diagram and Software . . . . .	49
3.2	Umbilical Connections . . . . .	49
3.2.1	Fluid Umbilicals . . . . .	49
3.2.2	Electrical Umbilical . . . . .	50
3.3	Temperature Condition System . . . . .	51
3.4	Mission Control . . . . .	52
3.4.1	Mission Control Box . . . . .	52
3.4.2	Antennas . . . . .	52
<b>4</b>	<b>Mission Concept of Operations Overview</b>	<b>53</b>
4.1	Arming of the System . . . . .	54
4.2	Abort Scenarios . . . . .	55
4.3	Thrust Curves . . . . .	55
4.4	Flight Simulation . . . . .	55
<b>5</b>	<b>Conclusions and Outlook</b>	<b>57</b>
	<b>List of Figures</b>	<b>59</b>
	<b>List of Tables</b>	<b>61</b>
	<b>List of Acronyms</b>	<b>62</b>
	<b>Glossary</b>	<b>64</b>
	<b>References</b>	<b>65</b>
	<b>Appendix A: System Data</b>	<b>67</b>
	<b>Appendix B: Detailed Test Reports</b>	<b>71</b>
B.1	Recovery System Testing . . . . .	71
B.1.1	Recovery System Electronics . . . . .	71
B.1.2	Ground Test Demonstration of Recovery System . . . . .	72
B.1.3	Flight Test Demonstration of Recovery System . . . . .	107
B.2	Hybrid Propulsion System Testing . . . . .	126
B.2.1	Hybrid Engine Ignition . . . . .	126
B.2.2	Static Hot-Fire Testing . . . . .	138
B.2.3	Hybrid/Liquid Propellant Loading and Offloading . . . . .	245
B.3	Proof Pressure Testing of SRAD Pressure Vessels . . . . .	248
B.4	Test of SRAD FC with Capability of actuating the Recovery Systems . . . . .	254
B.5	Additional Test Reports . . . . .	258
B.6	Explanation of overall Testing Strategy . . . . .	304



# 1 Introduction

## 1.1 Team Introduction and Overview

The ASTG was founded in late 2019 at the Graz University of Technology (TUG) as a non-profit organisation by a motivated group of students. Through the shared enthusiasm for the topics rocketry and aerospace, the team quickly grew to over 60 members in 2021 and nearly 80 in 2022. During this time multiple projects were carried out, most notably the participation in EuRoC 2021 with the rocket AVES and EuRoC 2022 with AVES II. Both times ASTG had successful launches and was able to win three awards in total. Only the successful recovery of the rockets proved to be a difficult goal to achieve. Still, lots of experience was gathered in those years and together with the hybrid Demonstrator, which was already designed and manufactured in parallel, this provided the foundation for the new project, HALCYON.

Overall, the team this year consists of 80 members from four universities. With very diverse fields of studies from all study levels, a good spectrum of different ages, and a steadily growing number of women, ASTG has the ability to take on even the most challenging projects and find new and innovative ways to solve problems. Figure 1.1 tries to highlight the diverse demographic of the team.

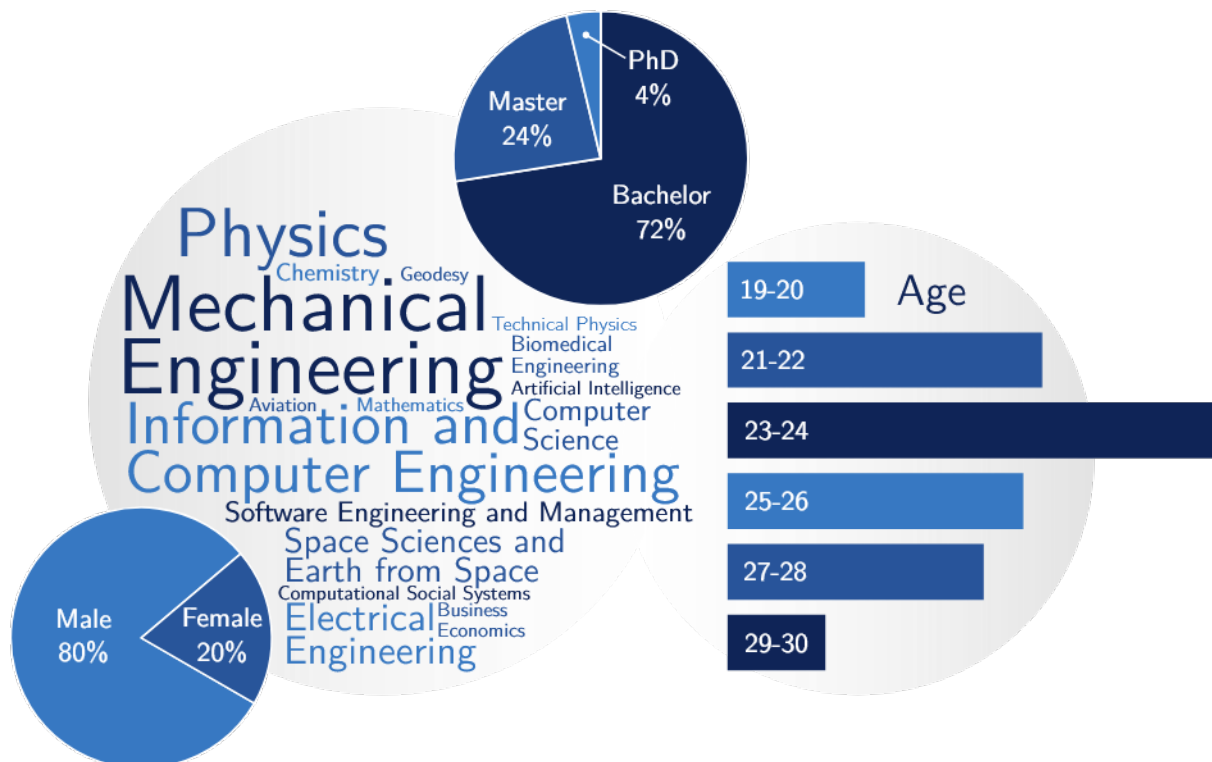


Figure 1.1: Overview of the team demographics showing study levels, gender distribution, the fields of studies, and age distribution.

## 1.2 Team Structure

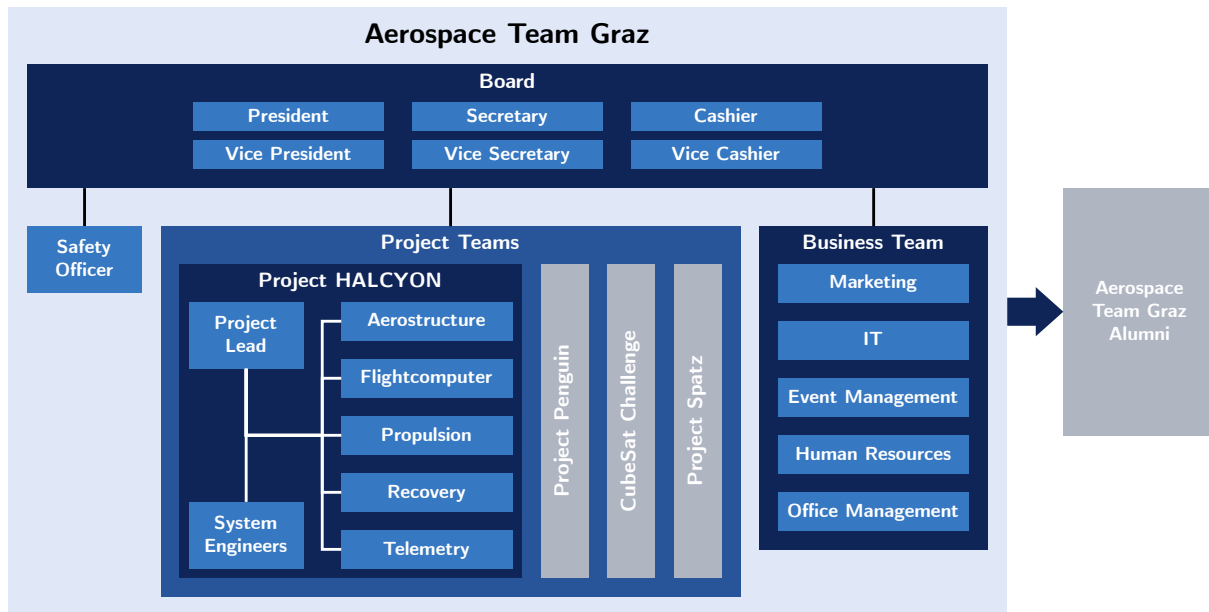


Figure 1.2: Organisational structure of the ASTG.

Figure 1.2 illustrates the organisational structure of the ASTG. Starting at the top, the Board is the elected leadership of the organisation, deciding on the most important matters and working to provide the necessary infrastructure and funds for the rest of the team. Together with the Business Team, they are also in charge of administrative tasks and public relations, e.g. Marketing, Event Management, and Human Resources.

On the technical side of things, the team is organised by the project they are working on. For HALCYON the Project Lead together with the System Engineers coordinates many aspects by ways of time-, resource-, interface-, and risk management, as well as helping with the documentation of the project.

Working groups or so-called modules are organised by the systems they design, engineer, program, and build. Starting with the Aerostructure module (AST), which combines aerodynamics and structure, works mainly on the airframe and all attachment points for the other systems. The Flightcomputer module (FLI) is tasked with designing and programming the Student Researched And Developed (SRAD) flight computer, the read-out of all sensors, and the control of all actuators inside the rocket and the Ground Support Equipment (GSE). Closely working together with FLI is the Telemetry module (TEL), which has the main task of providing the wireless data-links between Mission Control (MC), rocket, and GSE, as well as the Global Navigation Satellite System (GNSS) tracking of the rocket. To provide the power for getting off the ground, the Propulsion module (PRO) works on everything needed for the hybrid engine inside the rocket and the corresponding GSE to fill it up with oxidizer and pressurizing gas. Lastly, the Recovery module (REC) is responsible for the soft landing of the rocket, by designing and manufacturing the deployment systems and parachutes.

The Safety Officer oversees all groups to keep everyone safe when performing tests and handling hazardous substances.

## 1.3 Partners and Supporters

Even with the hard work from all the motivated team members, ASTG still relies on the cooperation with numerous partners and sponsors to realise demanding projects. The support comes from educational institutions, public funds, and businesses in many different forms, e.g. as monetary donations, supplying materials and tools, providing manufacturing capabilities, software licences, or contributing their know-how and giving us advice. Sponsors from this year include Graz University of Technology, European Space Agency (ESA) Space Solutions Austria, the Austrian Federal Ministry for Climate Action, Environment, Energy, Mobility, Innovation and Technology (BMK), the Institute of Manufacturing Engineering (IFT), the Institute of Innovation and Industrial Management (IIM), Astotec Pyrotechnic Solutions, Peak Technology, and over fifty more.

## 1.4 Project Goals

Our goals for project HALCYON are:

- Create high-quality and comprehensive technical documentation as a foundation for future projects.
- Advance the knowledge and experience for propulsion systems at ASTG by designing and building a pressurized hybrid engine.
- Carry out a test flight in Austria with the complete rocket and GSE, as the ideal preparation for Portugal.
- Keep up and strengthen the ASTG team spirit and sportsmanship while making new acquaintances from all over Europe.
- Reach the top five at EuRoC 2023.

## 1.5 Mission Objectives

The mission objectives for the launch vehicle are as follows:

- Carry a payload of 3x1U CubeSats with a total mass of 4kg to continue the efforts of getting secondary school students involved in rocketry and space sciences.
- Accomplish a successful launch to the target apogee of 3000m and achieve a safe recovery of HALCYON.



## 2 Launch Vehicle System Architecture

### 2.1 Overview

The various systems that make up the flight vehicle are partitioned among the five modules, as shown in Figure 2.1. The figure also depicts the tight integration of many different components, which required well-coordinated interfaces between the modules but allowed for mass- and space-efficient construction while still retaining a feature-rich rocket.

Starting at the nose cone, which contains the official altitude logging and tracking system on top of the 3x 1U CubeSat payload, and attaches to the rest of the airframe with a coupling tube secured by shear-pins. This is the point of separation used to deploy the recovery system, with its drogue- and main parachute.

Mounted right below the recovery system is the electronics mount, home to the flight computer and telemetry systems. Two wireless connections are implemented, one using patch antennas adhered to the outer hull, the other using an internal omnidirectional antenna. The flight computer controls all propulsion system actuators, collects various sensor data, and actuates the recovery deployments.

Next in line is the propulsion system, beginning with the nitrogen pressurization system, mounted to the top of the oxidizer tank together with the arming system, two radial facing cameras, and the nitrogen fill port. Made as a welded assembly, the oxidizer tank holds the nitrous oxide used in the hybrid engine and also serves as the structural component in this section of the rocket. Connected directly to the bottom of the tank are the servo-actuated main valve, a burst-disk to prevent overpressure, and a manual relief valve.

The last internal system is the combustion chamber, attached via a topology-optimized aluminium thrust structure. Utilizing a swirl injector, the nitrous oxide is brought into contact with the paraffin wax fuel, ignited by an internal rocket candy ignitor. The produced combustion gases are expelled through the graphite nozzle at the rear. The tail cone, with its four fins, covers the combustion chamber and improves the aerodynamic stability while also housing the downwards facing tail camera.

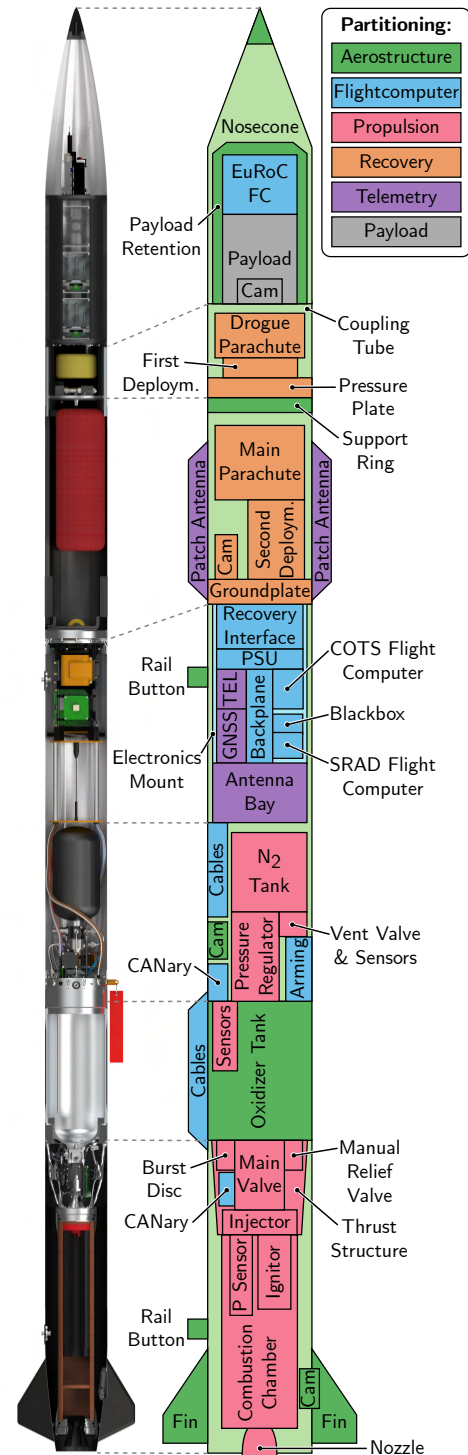


Figure 2.1: Overview of the launch vehicle and partitioning of major components.

## 2.2 Propulsion Subsystem

The propulsion system of HALCYON is a pressurized hybrid motor using liquid nitrous oxide ( $N_2O$ ) as oxidizer and nitrogen ( $N_2$ ) as pressurant gas. The choice of a pressurized hybrid engine was made to ensure constant thrust throughout the burn and to allow quicker fuelling and launch readiness.

During the development process, three oxidizers were considered: hydrogen peroxide, liquid oxygen and nitrous oxide. Nitrous oxide was ultimately chosen due to its ease of handling and availability. Several options were evaluated for the pressurant gas, including nitrogen, helium, argon, and pressurized air. Helium and argon were eliminated as viable options due to their benefits not justifying the higher cost. As pressurized air would have to be treated to ensure that no pollution and moisture enters the fluid system and nitrogen is readily available, nitrogen was chosen as the pressurizing gas. Although some hot-fire tests and the preliminary pressure tests with water for the injector verification were performed with compressed air. These tests showed the use of a filter for the oil residuals from the compressor and a drying agent for the moisture in the air being vital. Other than that, compressed air showed a similar thermodynamic performance to nitrogen, allowing it to be a workaround if no nitrogen is available.

The choice of fuel was between paraffin and Acrylnitril-Butadien-Styrol (ABS). For HALCYON, paraffin was chosen because it is cheap, easy to obtain in large quantities and easy to form into fuel grains by spin casting.

Table 2.1: Main rocket engine characteristics.

Characteristic	Value
propulsion stack length	1523 mm
nominal pressurant tank pressure	300 bar
nominal oxidizer pressure	66 bar
nominal operating combustion pressure	35 bar
total impulse	11 000 Ns
burn time	5 s
oxidizer mass	4200 g
fuel mass	1150 g
empty mass	9800 g

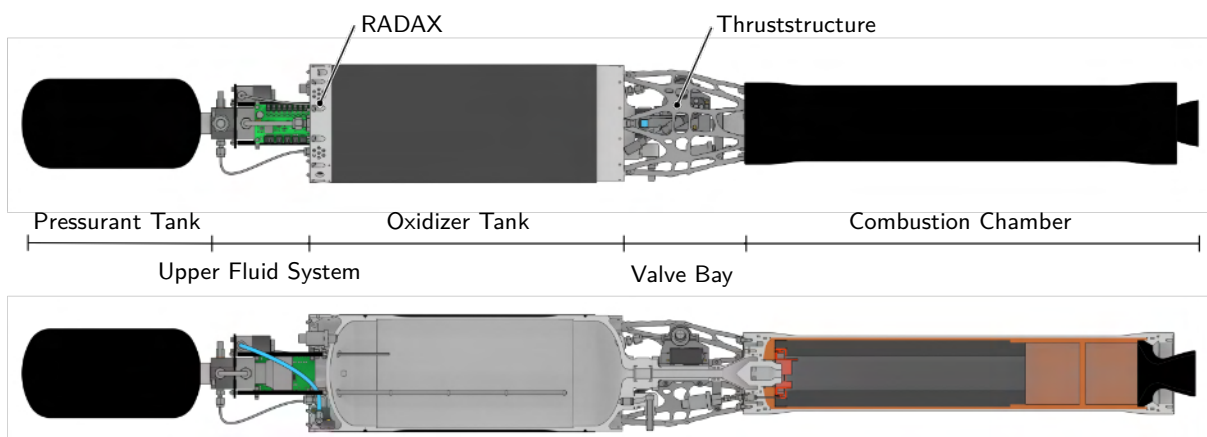


Figure 2.2: Overview of propulsion stack sections.

### 2.2.1 Fluid System

In a pressurized hybrid motor, the oxidizer is forced into the combustion chamber by a separate pressurant gas that is stored in an additional tank. A pressure regulator connects the pressurant and oxidizer tank. The pressure regulator keeps the oxidizer tank pressure constant during the burn, resulting in a stable thrust during the burn duration. After the burn, the inert pressurant gas extinguishes and cools the combustion chamber. Another benefit of the pressurized system is that the oxidizer can be stored at lower temperatures. Therefore, this system does not rely on the self-pressurizing properties of  $N_2O$ , which results in higher density and a smaller tank. For example, the density of  $N_2O$  at the target operating temperature of  $-10\text{ }^\circ\text{C}$  is 45 % higher than the density at  $32\text{ }^\circ\text{C}$  which equates to 66 bar in a self-pressurized system. Furthermore, as the system pressure is not dependent on the environmental conditions, a faster launch readiness can be achieved.

A design goal for the HALCYON hybrid engine was full instrumentation of all parts of the engine. This is to ensure mission control has every needed information about the state of the fluid system at all points during operation. For this purpose, the pressure is measured in the pressurant tank outlet, the oxidizer tank and the combustion chamber. In the  $N_2O$  tank, two pressure sensors measure both the liquid and gaseous phases. Temperature is measured at the  $N_2$  outlet and at four different positions inside the oxidizer tank using a multipoint thermocouple. Because the liquid  $N_2O$  is colder than the gaseous phase during tanking, the readings can be used to indicate the tanking level of the  $N_2O$ .

The fluid system of the rocket is connected to the filling station with two quick disconnects in the umbilical system, further detailed in Section 3.1 and Section 3.2.

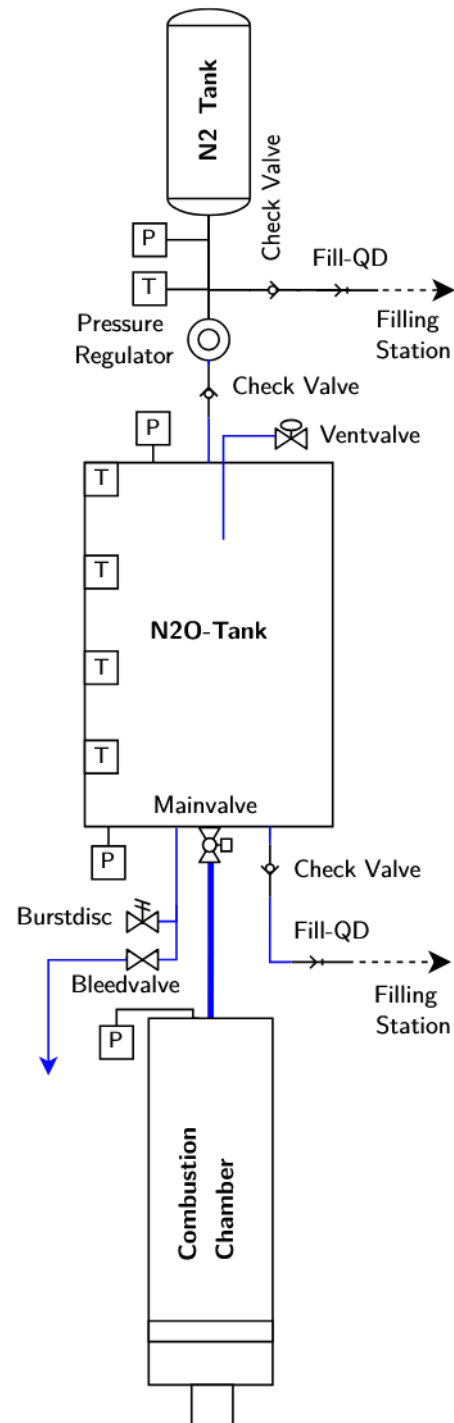


Figure 2.3: Fluid system of the Rocket.

#### Pressurant Tank

The pressurant tank stores the nitrogen used to pressurize the oxidizer system of the rocket engine. The amount of  $N_2$  has to be enough so that the pressure regulator can supply constant pressure in the oxidizer tank for the complete duration of the engine burn. When taking the temperature drop of the expanding gas into account, it was calculated that 1.2 L of nitrogen with

an initial pressure of 300 bar would be sufficient for the pressurization process. Ultimately a larger 1.5 L COTS paintball tank was chosen to ensure almost the same behaviour with an initial pressure of only 250 bar, making the system more tolerant to pressure drops. The Composite Overwrapped Pressure Vessel (COPV) is a type 4 vessel with a Polyethylene Terephthalate (PET) liner, making it one of the lightest COTS tanks available.

### Pressure Regulator

The pressure regulator's primary function is to reduce high pressure  $N_2$  to a lower pressure, ensuring that the oxidizer tank maintains a constant pressure during combustion. In most applications, the inlet pressure to the regulator is relatively constant, which allows the flow to be calculated as being temporarily constant during any design process. As our application experiences a significant drop in pressure from the high-pressure tank, the maximum flow will also change due to its direct correlation with the pressure drop and corresponding  $C_V$  value of the pressure regulator. The pressure reducer selected possesses a  $C_V$  value of 0.06 and features a piston design that allows a maximum inlet pressure of 414 bar and a maximum static outlet pressure of 80 bar. Rigorous testing was conducted to characterize the behaviour of the pressure regulator. As we have decided against a separate pressurant valve due to weight and complexity reasons, the nitrogen filling process directly pressurizes the whole system. To avoid any problems with the supply pressure effect, the filling process must be fast enough to overcome the lag of the pressure regulator and achieve a stable pressure in the oxidizer tank.

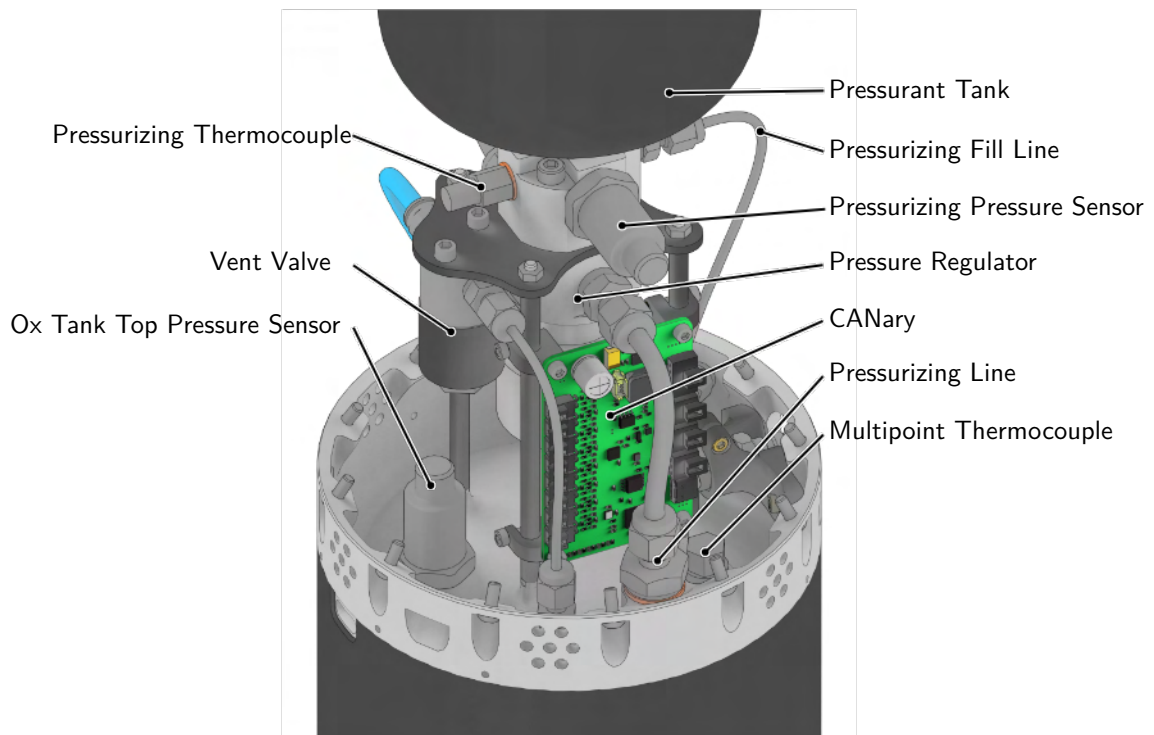


Figure 2.4: Upper fluid system excluding cameras, arming system and electrical umbilical.

### Oxidizer Tank

The oxidizer tank stores the  $N_2O$  for the rocket engine. It has a maximal capacity of 5.5 L. Besides the connection to the pressurant system and the main valve, three additional valves are integrated into the tank. On top, a vent valve with a dip tube is mounted. The length of the dip tube is used to determine the fill level of the tank during tanking. If the level of the liquid  $N_2O$  phase reaches the dip tube, liquid  $N_2O$  starts to flow through the vent valve, which serves as a

visual indicator. Additionally, the weight of the rocket is monitored, and the temperature at 25 %, 50 %, 75 %, and 100 % fill level is measured using a multipoint thermocouple. On the bottom of the tank, a burst disc with a burst pressure of 85 bar  $\pm$ 5 % prevents the oxidizer pressure from reaching critical levels. A manual relief valve is placed in the valve bay to release all pressure inside the propulsion system in the case of an electronics failure. This valve can be opened with a screwdriver while the rocket is vertical on the launch rail. Furthermore, the oxidizer quick disconnect is mounted to the lower bulkhead with the check valve directly screwed into the bulkhead. The oxidizer tank was designed as part of the load-bearing rocket structure and is therefore further detailed in Section 2.3.6.

### Main Valve

The Main valve is a 3-piece 1/2" ball valve. Due to space and weight savings, the COTS flanges of the valve are fully integrated into our system. The upper flange is included in the aluminium bulkhead of the oxidizer tank, while the lower flange, made out of EN AW 6082 T6 alloy, connects the valve to the combustion chamber via a feedpipe. This highly integrated design saves over 50 % weight in comparison to COTS components. The valve is actuated by a servo using a four-bar linkage. This four-bar linkage provides variable transmission with the highest transmission ratio at the end positions, which helps to overcome the breakaway torque. The position of the valve is monitored with a potentiometer directly connected to the shaft of the ball valve.

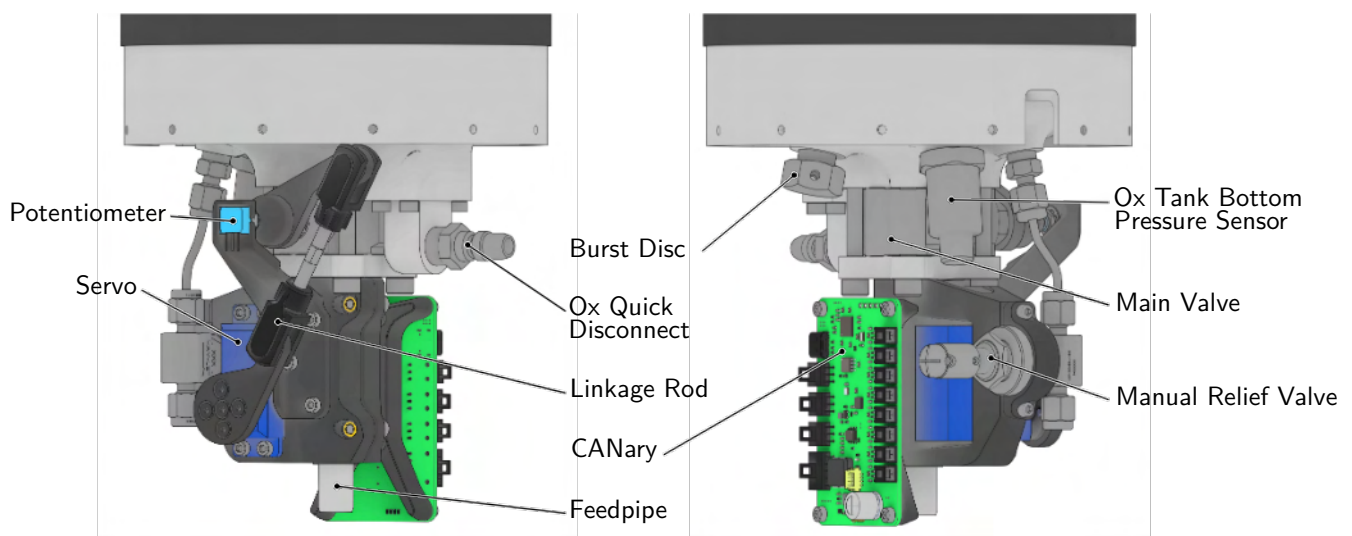


Figure 2.5: View of the Valvebay section.

## 2.2.2 Combustion Chamber

### Structure

The main structure of the combustion chamber is an aluminium tube of EN AW 6082 T6 alloy. This alloy was chosen for its high strength, therefore reducing weight. On each end of the combustion chamber, a tight fit for the O-Ring and a M100x2 internal thread is integrated to seal the combustion chamber and absorb the axial forces generated by the combustion pressure. Retainer rings are screwed in on these internal threads, holding the internal structure together. An aluminium nozzle holder secures the self-supporting graphite nozzle via a conical interface, which not only transmits the force but also seals the combustion chamber with the additional use of graphite paste. A CFD analysis of the combustion gases inside the nozzle provided

pressure and shear data, which then were used as loads in a FEA for the nozzle. In Figure 2.6, a cross-section of the nozzle assembly can be seen. When assembled, the nozzle presses against the post-combustion chamber insulation, which is glued into the main insulation.

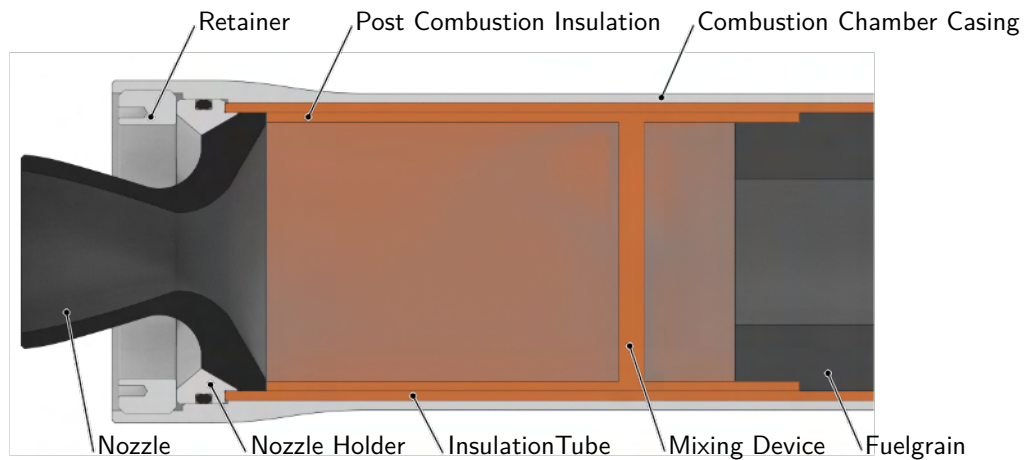


Figure 2.6: Detailed view of the nozzle section.

On the opposite side of the combustion chamber, a bulkhead, also made from EN AW 6082 T6 aluminium alloy, ensures the tightness of the combustion chamber but also contains the injector and an opening for a pressure sensor. The bulkhead is also weight-optimized with an elliptic shape on the inside. The bulkhead insulation is milled from phenolic cotton with the negative form of the bulkhead.

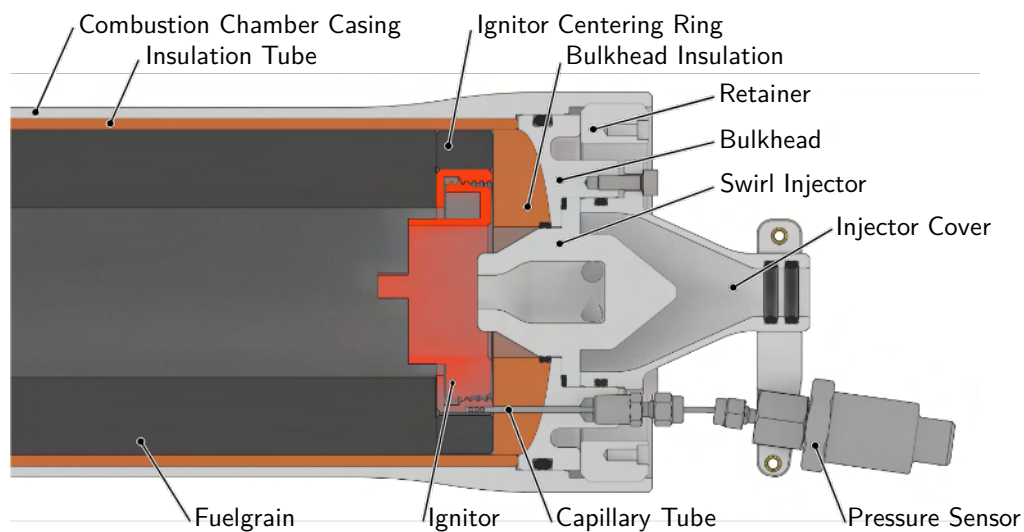


Figure 2.7: Detailed view of the bulkhead section.

## Injector

The primary function of an injector in a hybrid rocket is to atomize the liquid oxidizer as effectively as possible, preparing it for its reaction with the fuel grain. Comparisons in different literature (e.g. Heydari et al. [1]) suggest that swirl injectors offer significant advantages over impingement and showerhead injectors in terms of overall engine efficiency. For this reason, we developed a swirl injector for our Demonstrator engine, further detailed in Section 2.2.4, and improved the design since then. The swirl injector generates a regulated swirling motion of the oxidizer into the combustion chamber, thereby improving the mixing process. This is done by four tangentially arranged orifices that force the liquid into a swirling flow. As the oxidizer

spirals inward, a vortex-like effect at the injector's centre is created. At the lower end of the swirl injector, the fluid is accelerated in the axial direction and forced through a nozzle, expelling the droplets at the desired angle with an induced angular spin. During the development process, a range of water and cold-flow tests were conducted to achieve the desired flow rate, spray angle and pressure drop. The injector is made from aluminium using Selective Laser Sintering (SLS) 3D printing to facilitate the manufacturing of the complex geometry.

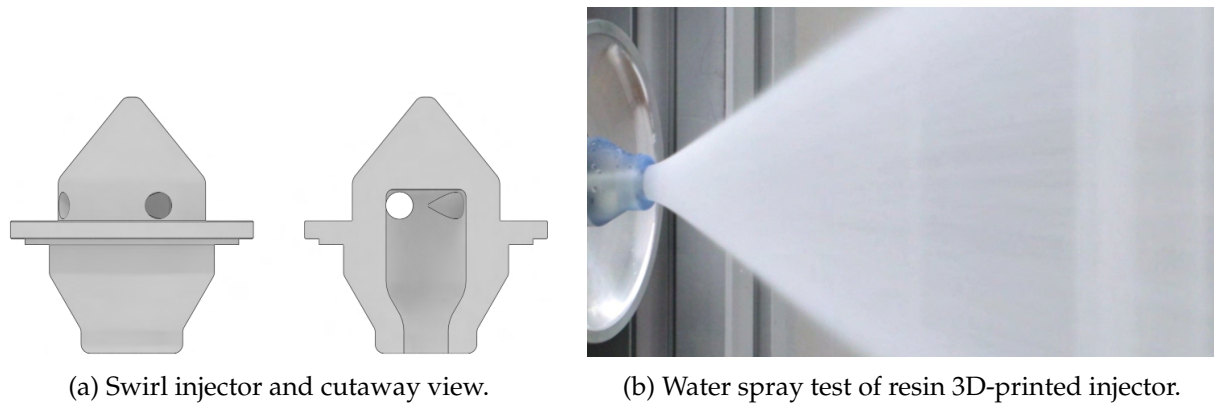


Figure 2.8: The 3D-printed aluminium swirl injector utilizes four tangentially aligned holes to create a swirl in the nitrous oxide flow.

### Fuel Grain

The fuel grain is cast directly into the phenolic resin cotton insulation, forming a hollow cylinder as seen in Figure 2.6 and Figure 2.7. It consists of 78 % paraffin wax, 20 % Ethylen Vinyl Acetate (EVA) and 2 % coal powder. The EVA improves the mechanical properties of the fuel; tests found that 20 % were the best compromise. Coal powder is included to improve the absorption of thermal radiation. To manufacture the fuel grain, the insulation tube is filled with the molten fuel and then spun at high speeds using a lathe. This spin-casting manufacturing process does not suffer from voids forming within the fuel grain while it cools down like other casting methods.

### Mixing Device

The function of a mixing device is to generate turbulences in the combustion gas, enhancing the intermixing between  $N_2O$  and paraffin droplets. Evidently, this leads to an increase in combustion efficiency [2]. It is made of phenolic resin cotton and consists of an outer ring and an inner plate connected by four radial struts. The area of the holes was designed to be slightly larger than the port area of the fuel grain to prevent a significant pressure drop. The mixing device is placed 1/4 of the length of the post-combustion chamber away from the fuel grain, as depicted in Figure 2.6.

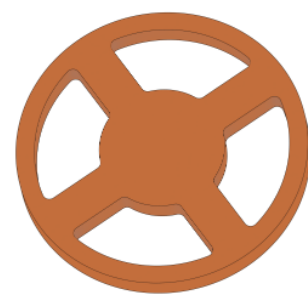


Figure 2.9: Mixing Device model.

### 2.2.3 Ignitor

The ignition is achieved with a pyrotechnic ignition device dubbed the "Screw Ignitor". Based on a 3D-printed structure, the ignitor is inserted at the top of the combustion chamber and secured by the bulkhead insulation, as seen in Figure 2.7. To accommodate the central injector, a ring design was chosen, which further provides a constant burn rate and cannot be extinguished or even thrown out by the expanding  $N_2O$ .

The print consists of two separate parts secured together using a thread, this design element doubles as a means to compress the pyrotechnic mixture. The pyrotechnic mixture contains 60% rocket candy made from 35% sorbitol and 65%  $\text{KNO}_3$ , 25% calcium silicide and 15% magnesium powder, resulting in a well workable mixture which produces masses of hot sparks after ignition. To achieve a fast and reliable ignition, an ignition accelerator coined Liquid CaSi was added to the inside of the 3D-print. A cut-out in the 3D-print further allows clearance for the pressure sensor in the combustion chamber, which is separated from the pyrotechnic mixture by two insulation chambers to prevent interference. Repeat testing showed the reliability of the system, as no instance of a failed ignition occurred.

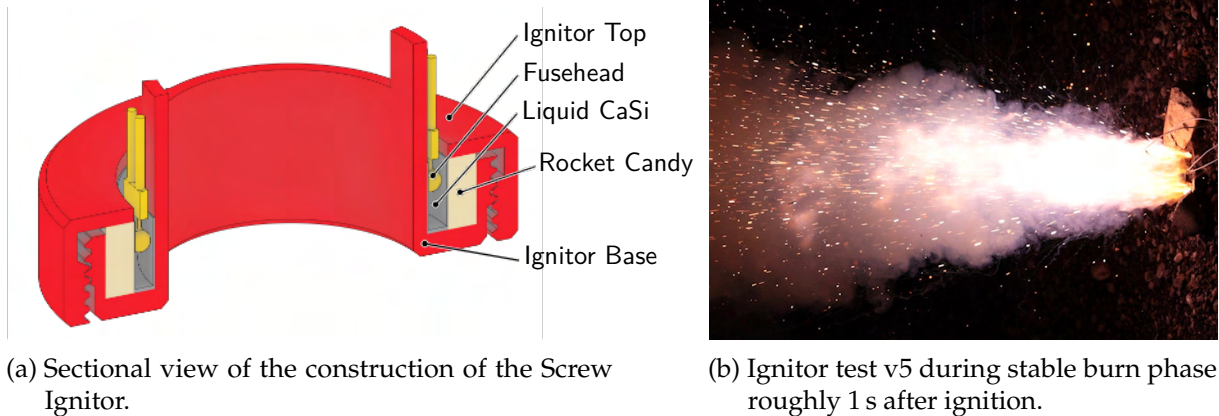


Figure 2.10: The Screw Ignitor proved reliable in numerous tests as no ignition failure occurred.

## 2.2.4 Propulsion Testing

To get a reliable propulsion system, an extensive testing campaign was necessary. The first step was to build and test a smaller-scale prototype hybrid engine. This engine, simply coined Demonstrator, is a self-pressurized nitrous oxide, paraffin hybrid engine with a peak thrust of 900 N, a total Impulse of 5100 Ns and a burn time of 6 s. As Demonstrator was the first hybrid rocket engine of the ASTG, it was used to test a multitude of designs for HALCYON. Demonstrator used a scaled-down version of the same swirl injector as HALCYON. It also provided initial experience with the handling of  $\text{N}_2\text{O}$  and the first fuel grain manufacturing tests were conducted. Demonstrator was successfully used in two cold-flows and one hot-fire test.

Next, a series of horizontal cold- and hot-fire tests were conducted. For these, the horizontal solid engine test stand Penguin was adapted to support hybrid rocket engines. During these tests, a simplified preliminary filling station was used. The main purpose of the horizontal tests was design verification and further engine development. In total, six horizontal hot-fires with additional cold-flows for testing of the tanking procedure were done.

The next testing phase was a series of vertical tests. In these tests, the final HALCYON hardware was tested. This includes the rocket engine, filling station, flight computer and ground support equipment. For these tests, a new vertical test stand was built. During the first set of tests, the propulsion stack was mounted directly to the test stand and for the remaining tests, the propulsion stack was fully integrated into the rocket.

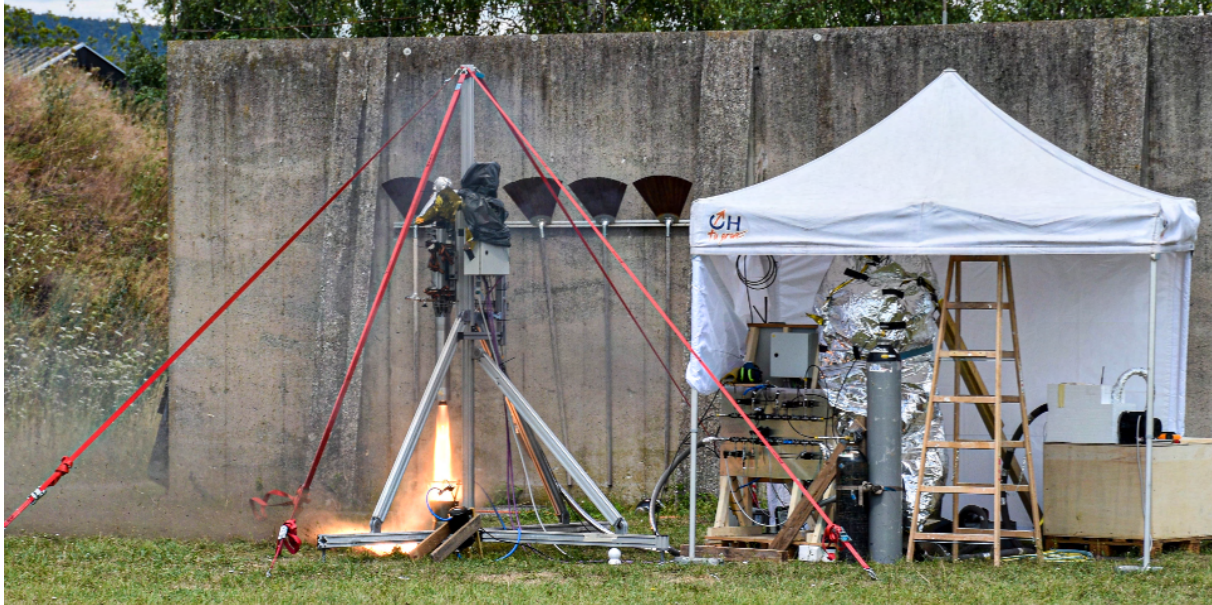


Figure 2.11: Vertical hot-fire test with the propulsion stack directly mounted onto the test stand.

The final testing milestone of the propulsion system was the flight test of the rocket. Due to the regulations at the testing site, a reduced oxidizer loading of 2.2 kg  $N_2O$  and 0.6 kg fuel was used to keep the total launch mass below 25 kg and reach a target height of 1500 m. In total, the hybrid engine was hot-fired eight times, including the test flight. A summary of all HALCYON hot-fires is given in Table 2.2. Note that HF 2.1, HF 4.2 and HF 5.1 had to be aborted due to problems, therefore not being listed.

Table 2.2: Summary of HALCYON hot-fire results.

Test ID	peak thrust	total impulse	oxidizer mass	burn time
HF 1.1	2283 N	5568 Ns	2.4 kg	2.2 s
HF 2.2	2236 N	9946 Ns	4.2 kg	4.5 s
HF 2.3	2568 N	7807 Ns	3.2 kg	3.5 s
HF 3.1	2127 N	10 323 Ns	4.2 kg	5 s
HF 3.2	2374 N	11 466 Ns	4.2 kg	5 s
HF 3.3	2363 N	11 390 Ns	4.2 kg	5 s
HF 4.1	3042 N	10 516 Ns	4.2 kg	3.4 s
FT 1	2817 N	5310 Ns	2.2 kg	2.1 s

## 2.3 Aerostructure Subsystem

Overall, the structure of HALCYON is based on a load-bearing, composite outer shell, with the goal to be as light and space-efficient as possible. In total, there are five outer sections, these being the Nose Cone Section (NC-S), Recovery Section (REC-S), Avionics Section (AVI-S), Oxidizer Tank Section (OT-S) and Tail Section (T-S).

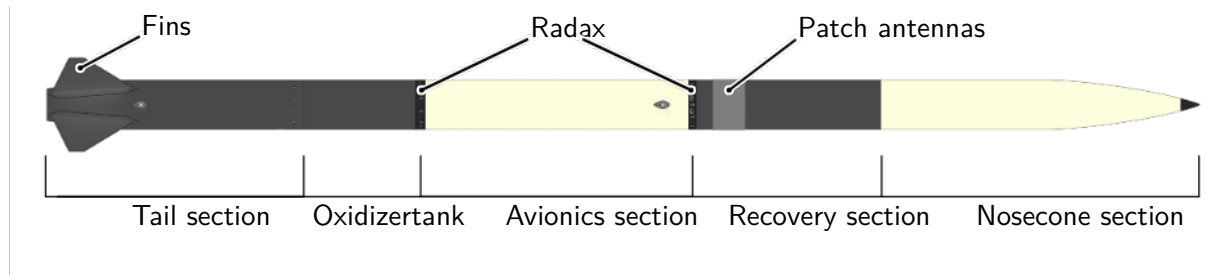


Figure 2.12: Overview of airframe with different sections and some key features.

One main driving design factor was the easy integration of internal subsystems, achieved through multiple connection points. Linked by Radax joints are the oxidizer tank, AVI-S and REC-S. Meanwhile, the Coupling Tube (CT) provides the connection between the NC-S and the REC-S, while the T-S is mounted on the rear end of the oxidizer tank.

The loads acting on the airframe were calculated for ten different load scenarios, including handling, on launch rail, flight plus side wind and drogue deployment (??).

### 2.3.1 Shell

The shell is made of composite material tubes wrapped layer by layer around a mandrel. For sections that need to be radio transparent (NC-S, AVI-S), a mixture of glass fibre, Poly(p-phenylene-2,6-benzobisoxazole), Zylon<sup>®</sup> (PBO) and ceramics was the reinforcement of choice. The remaining sections (REC-S, OT-S, T-S) are made of Carbon Fibre Reinforced Polymer (CFRP).

Classical lamination theory was used to confirm the structural integrity under the loads shown in ???. The calculations were done by a student-written script. To confirm the results, Altair ESAComp<sup>™</sup> was used. With the material properties provided by the manufacturer, the final Lay-Up was determined.

Table 2.3: Properties of airframe winded tubes.

Section	Material	Lay-up [°]	Shell Thickness
NC-S	GFRP/CeFRP	(85,-10,10,-10,10,-10,10,-10)	1.21 mm
CT	CFRP	(85,-10,10,-10,10,-10,10,-10)	1.56 mm
REC-S	CFRP	(85,-85,10,-10,10,-10,10,-10)	1.3 mm
AVI-S	GFRP/PBO/CeFRP	(85,-85,10,-10,10,-10,10,-10)	1.25 mm
OT-S	CFRP	(85,-85,10,-10,10,-10,10,-10)	1.3 mm
T-S	CFRP	(85,-10,10,-10,10,-10,10,-10)	1.3 mm

### 2.3.2 Aerodynamics

To determine the aerodynamic characteristics of our rocket, many Computational Fluid Dynamics (CFD) simulations were performed, which accumulated roughly 20000 CPUh of simulation time. These simulations were mainly used to determine the drag coefficients of the rocket during the boost and coast phase.

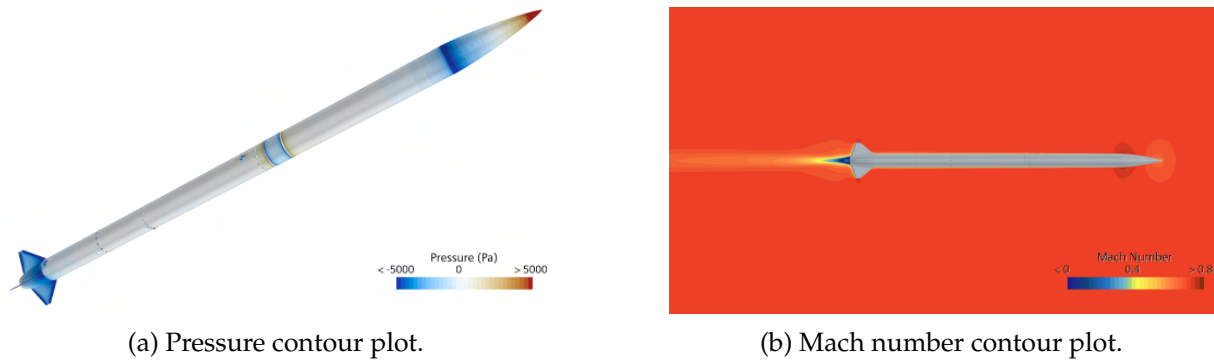


Figure 2.13: Results of the CFD simulation at Maximum Dynamic Pressure (Max Q).

#### Nose Cone and Tail Cone

In an attempt to minimize drag in subsonic conditions, the nose cone and tail cone are a revolve of a curve based on the Haack Series with  $C = 0$ . Applying this geometry to not only the nose cone but also the aft part of the rocket helps to reduce drag further. This was confirmed by the aforementioned CFD simulations.

The detachable nose cone tip was engineered from aluminium to endure aerodynamic forces and maintain a precise aerodynamic profile, a feat unattainable through a completely filament-wound NC-S. Once the payload is integrated, the NC-S is mounted onto the CT, explained in Section 2.3.4.

Enabling easy integration, the T-S can be pushed over the propulsion stack up to the oxidizer tank, where it is attached with radial screws.

Sitting between two fins, the outer cover of the camera assembly (Figure 2.14) is adhered to the shell while the rest is mounted on the interior. One major goal of the design was to not significantly increase the cross-section.

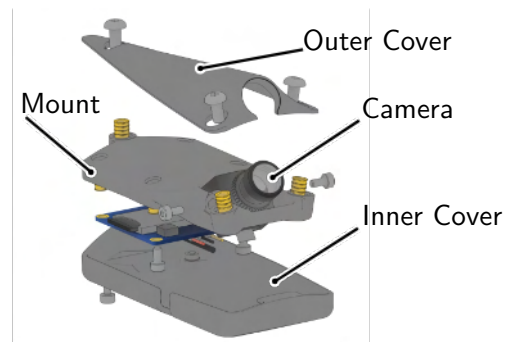


Figure 2.14: Tail camera assembly with 3D-printed mount and camera parts.

#### Fins

The fins for HALCYON have a trapezoidal shape, designed to be attached to the curved part of the T-S tube. With a thickness of 5 mm, they are positioned and sized to guarantee the rocket's stability up to wind speeds near 10 m/s.

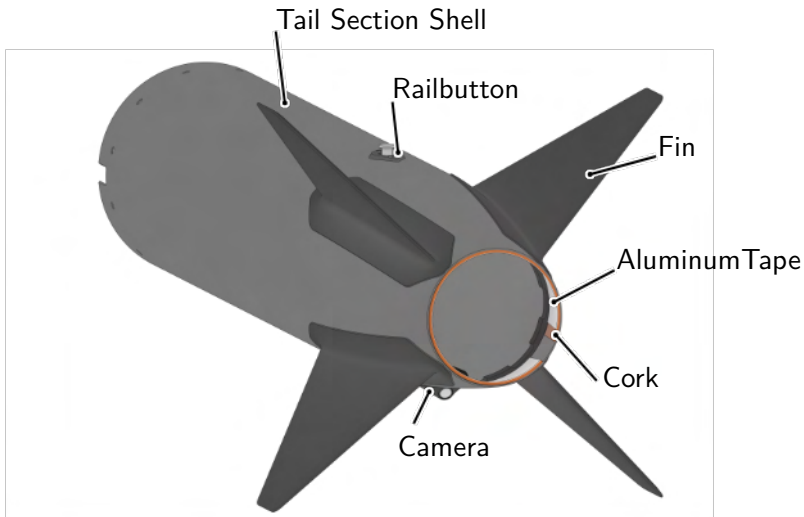


Figure 2.15: Rear view of the fins and T-S.

### 2.3.3 Payload Structure

The nose cone shell serves as the enclosure for the 3U CubeSat payload and the Commercial Off The Shelf (COTS) flight computer, Control And Telemetry Systems (CATS). The payload and the flight computer are affixed to four rails made from 3D-printed Polylactic Acid (PLA) material. This design facilitates the seamless integration of these subsystems by sliding them into the NC-S. Along the axial direction, the loads are transmitted to two load-bearing CFRP rings at the front and rear of the payload stack. These CFRP rings are securely attached to the shell using epoxy adhesive.

Supporting the payload stack at the rear is the payload retainer with an isogrid structure on the surface, fastened to the lower CFRP ring using eight screws. The retainer not only offers support but also forms a seal between the pressure chamber and the nose cone. It additionally incorporates a stainless steel swivel for connecting the nose cone to the drogue chute and an acrylic glass window to afford the lower CubeSat an unobstructed view of deployment occurrences.

To ensure the retainer's structural integrity, a Finite Element Analysis (FEA) was conducted, shown in Figure 2.17. This analysis aimed to verify the plate's capability to endure pressurization forces while reducing weight.

A prepreg Lay-Up with two negative mold halves was used to manufacture the fins. Three layers on each half join and overlap at the edges, with the orientation being  $[0/30/60/\text{CORE}/60/30/0]$ . A Polyurethane (PU) foam core fills the inner gap, adding stability while being lightweight. Integrated into the fin shape is a flange, which is adhered to the T-S shell using 3M<sup>TM</sup> Scotch-Weld<sup>TM</sup> DP 490.

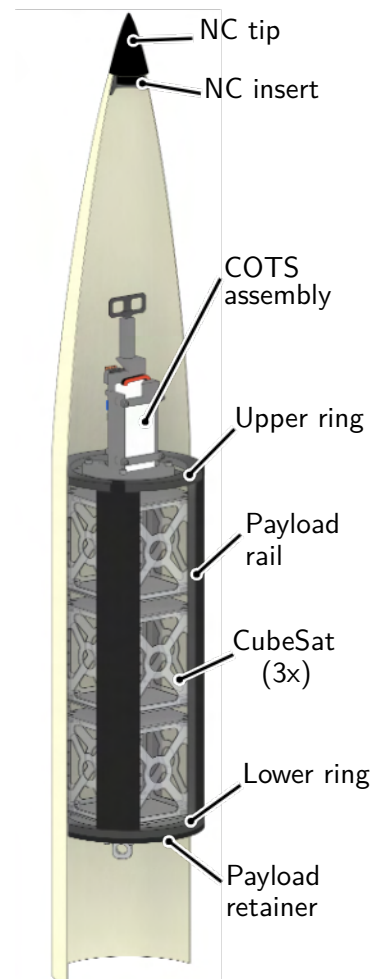


Figure 2.16: Sectional view of the NC-S with the payload section.

### 2.3.4 Coupling Tube and Pressure Chamber

The separable linkage between the NC-S and REC-S is achieved through the utilization of a CFRP Coupling Tube (CT), which is affixed to the REC-S through adhesive bonding. The NC-S's secure positioning is facilitated by this tightly fitting tube, in addition to three M2.5 nylon shear bolts. The pressurized chamber, formed by an aluminium plate at the rear and the payload retainer at the front, is pressurized using the initial deployment system, responsible for expelling the nose cone at its apogee. Axial support for the plate is provided by a CFRP ring that is bonded into the CT, which has a wall thickness of 1.5 mm.

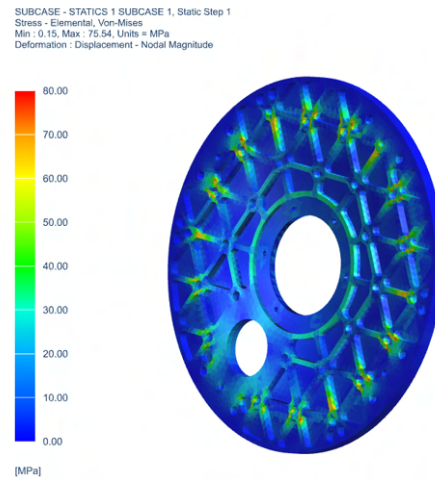


Figure 2.17: FEA results for the payload retainer.

### 2.3.5 Radax

The individual sections of the rocket are fixed together by so-called Radax joints, consisting of two aluminium halves bonded to their respective shell section with epoxy adhesive. The joint is held together by twelve M4 screws, with a conical interface between the two halves to allow self-centering while also providing alignment when tightening the screws. The preload ensures that under load the joint is still under compression, which prevents play and increases operational stiffness. Moreover, additional material removable between the screw locations could be realized with the help of FEAs, further decreasing the weight.

Compared to alternatives like radial screws, bayonet- or V-band-connections, the Radax joint takes up little inner space at the connection, thus allowing integration of large internal assemblies, such as the fluid system, while still maintaining high joint stiffness under load, and low weight.

Integrated mounting points are another advantage, with the Radax parts allowing for additional internal mounting points, such as the ones discussed in Section 2.3.6.

Stresses and bolt forces for all load cases were determined through a multi-step FEA of the joint. These results were subsequently employed to verify the connection's compliance according to VDI-2230 standards.

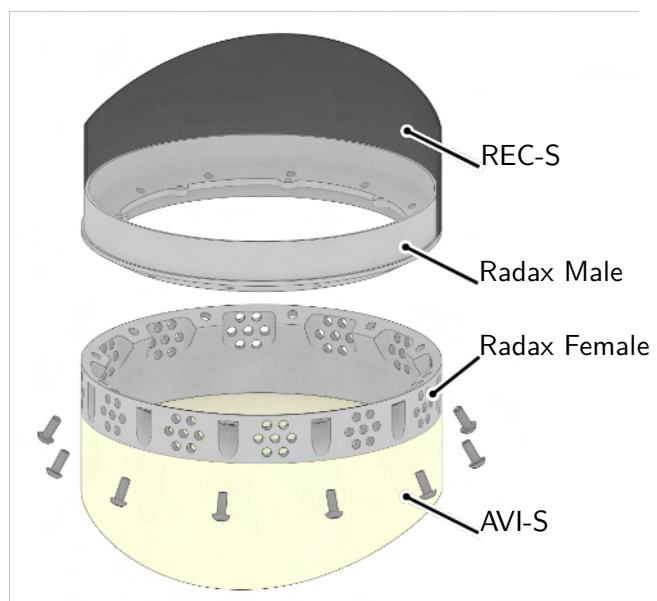


Figure 2.18: Radax joint between AVI-S and REC-S.

### 2.3.6 Oxidizer Tank

The 5.5 L oxidizer tank, built to contain pressures of up to 66 bar, was designed with integration of mounting points in mind, with the additional goal of having a load bearing structure.

The tank consists of three main parts: the two end caps and a cylindrical middle section. All are made of the alloy European Norm (EN) Aluminium Wrought (AW) 6082, which exhibits high strength relative to most other aluminium alloys and is suitable for welding.

Considering these design objectives, a welded three-part aluminium tank with a diameter close to that of the rest of the rocket became the preferred option.

With the help of FEAs, a minimum wall thickness of 3.4 mm was determined, which was applied to most of the cylindrical section. The walls are thicker at the ends of the cylinder and on the bulkheads, which have an ellipsoid shape. This geometry was selected due to being stronger than a flat end and more space efficient than a hemisphere.

Tungsten Inert Gas (TIG) welding was chosen as the welding process with an AlSi<sub>5</sub> (S AL 4043A) filler wire. A U-shaped welding seam helps ensure easier access to all areas of the seam while allowing it to be deep enough.

After the welding process, a small amount of the outer diameter near the welding seam is removed, which had been intentionally manufactured slightly larger than the final diameter. This helps even out the welding seam to reduce the local notch effect, thus improving structural integrity.

To reduce the number of necessary components, many mounting points were integrated into the top and bottom of the tank. Included at the top is the female piece of the Radax joint, below which lie multiple radial screw holes on the circumference for attaching various electronics. Furthermore, the ellipsoid shapes provide threaded holes for all of the fluid system's directly mounted components. There are also holes for the oxidizer quick disconnect and electrical umbilical.

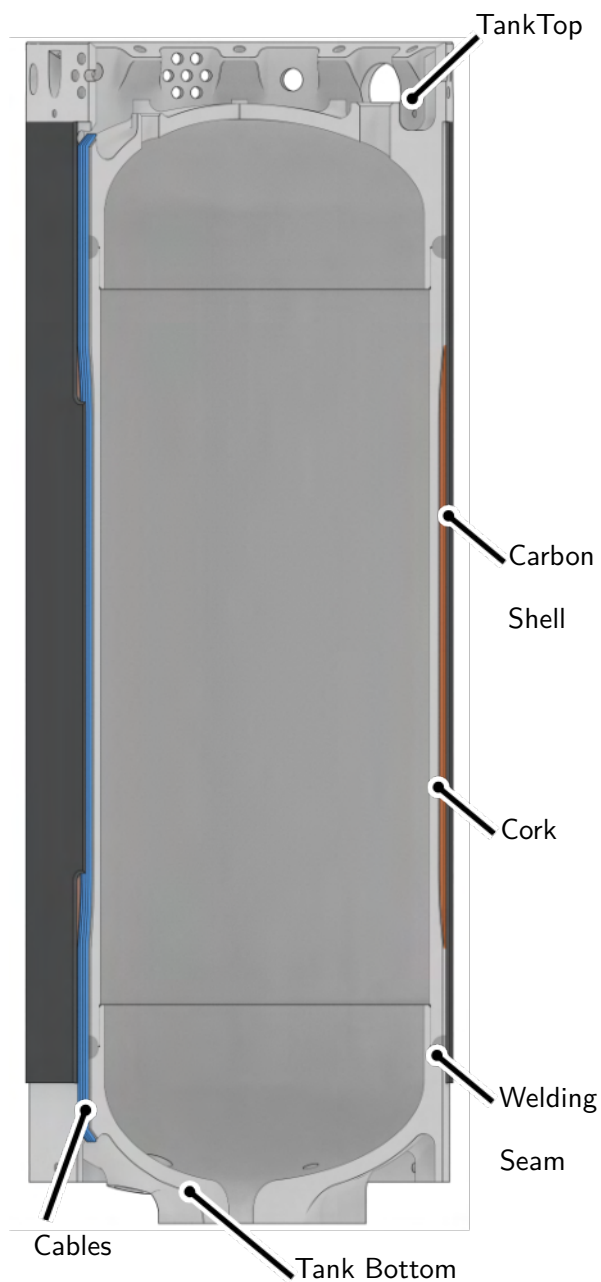


Figure 2.19: Oxidizer tank structural overview.

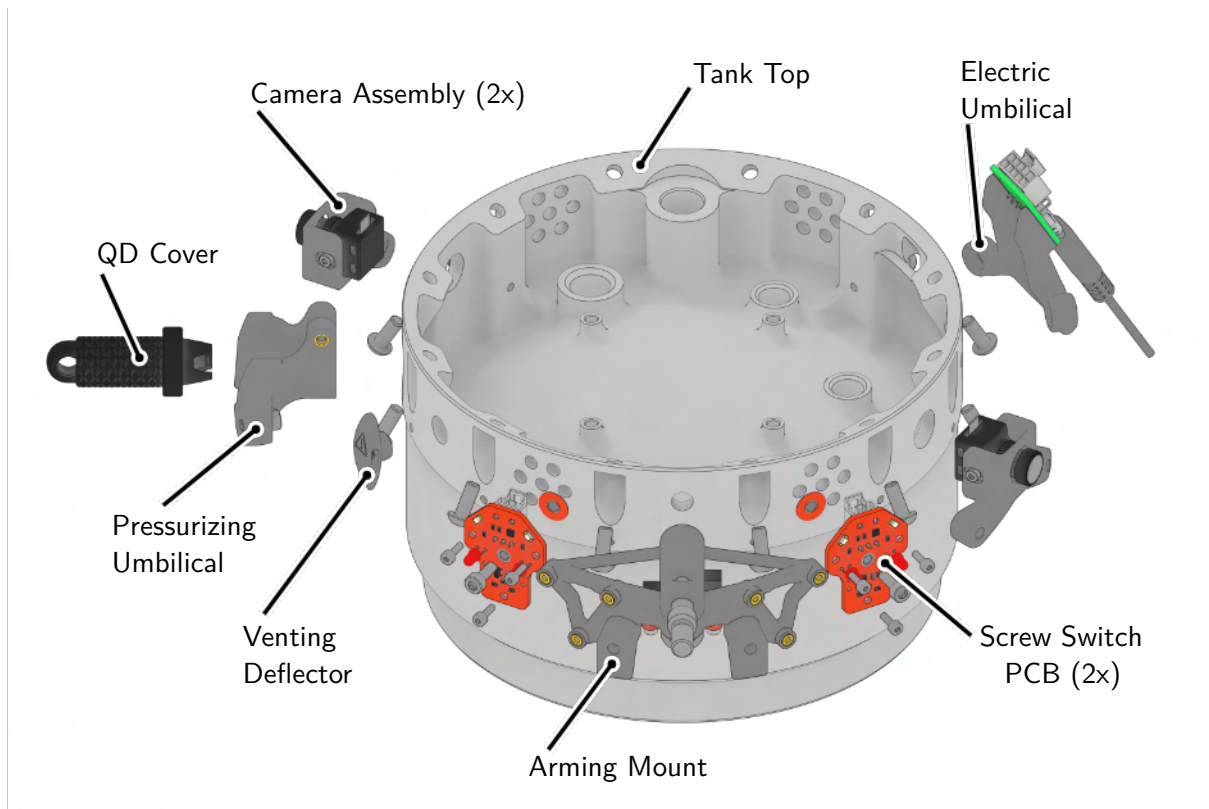


Figure 2.20: Oxidizer tank top with integrated Radax and mounting points.

The outer surface of the ellipsoid shape includes threaded holes for all of the fluid system's directly mounted components, detailed in Section 2.2.

Due to the significant temperature differences between the  $N_2O$  and outside of the tank, insulation is necessary. This comes in the form of a thin cork layer directly on the aluminium cylinder surrounded by a carbon tube on the outside to match the rest of the hull. To insulate the ends and prevent the build-up of condensation and subsequent ice, a self-adhesive insulation material (ArmaFlex<sup>®</sup> XG) was glued to the open surfaces.

### 2.3.7 Thrust Structure and Motor Retention

The purpose of the thrust structure (shown in Figure 2.21) is to facilitate the transfer of loads from the combustion chamber onto the tank, which serves as a load-bearing structure, and subsequently distribute these loads across the entirety of the rocket.

The build volume is defined by the space taken up by the lower fluid assembly at the bottom of the tank, as well as the outer rocket diameter. All major loads were taken into consideration, these being primarily the axial and shear forces, as well as the bending moment.

It is firmly attached to both the tank and the combustion chamber's upper retainer using six bolts on each side. Since the design of the thrust structure was topology optimized in order to reduce weight while maintaining the necessary strength, 3D-printing aluminium was chosen as the manufacturing process.

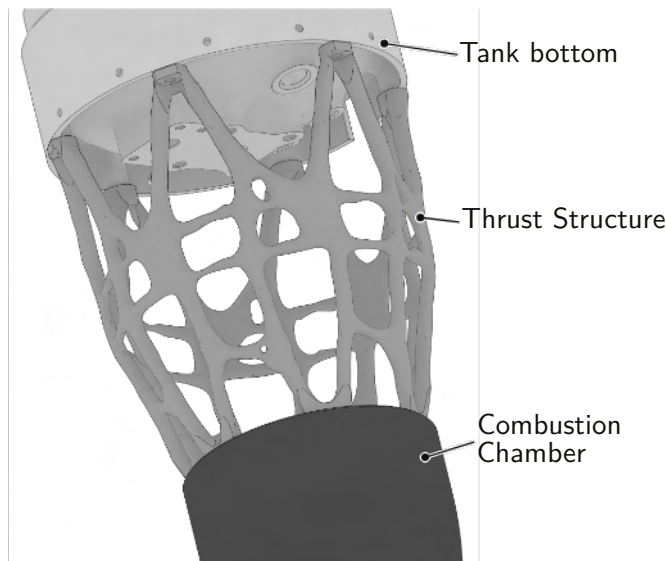


Figure 2.21: Thrust structure between tank and combustion chamber.

### 2.3.8 Retractable Railbutton

The connection to the launch rail is established using a pair of retractable railbuttons. These railbuttons are equipped with spring-loaded mechanisms that retract the guides upon departure from the launch rail, reducing protrusions from the hull. Positioned near the rocket's Center of Gravity (CoG) and rear section, these connections help minimize stress on the rocket while providing a longer period of guidance compared to locations closer to the tip. Mounting the railbuttons involves attaching an internal aluminium component to the carbon tubes of the rocket, achieved through the use of epoxy adhesive.

A custom SLS 3D-printed glide surface (I8-ESD) with high abrasion resistance is attached to the exterior surface, ensuring smooth movement at high speeds. Additionally, the guides are coated in Polytetrafluoroethylene (PTFE), further reducing the friction of the surfaces in contact with the launch rail.

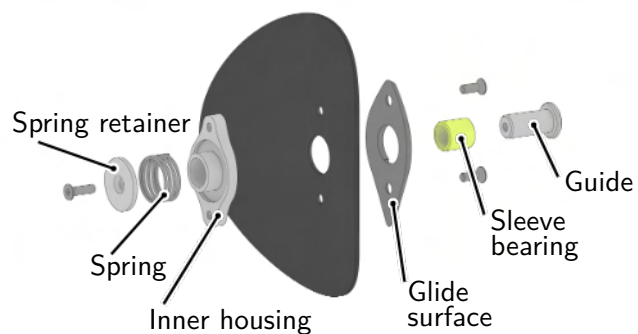


Figure 2.22: Exploded drawing of Railbutton assembly.

## 2.4 Recovery Subsystem

For recovery, a dual deployment system with two separate parachutes is used, as depicted in Figure 2.23. At apogee, the first deployment system separates the nose cone and ejects the drogue parachute to stabilize the rocket. The drogue and all its load-bearing components are designed to withstand an opening at speeds of at least 100 m/s. The main parachute is deployed at an altitude of 450 m by the second deployment to ensure a safe landing without damaging any components.

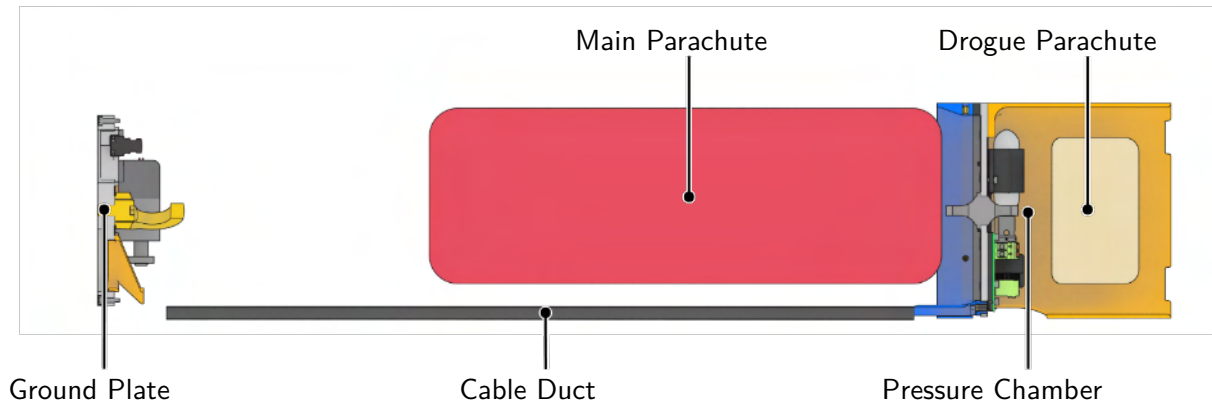


Figure 2.23: Sectional view of the whole recovery system.

### 2.4.1 First Deployment

The purpose of the first deployment is to separate the nose cone by pressurizing the pressure chamber and shearing off three M2.5 polyamide shear pins. The chamber is fully sealed except for the required ventilation hole. In the calculations, the escaping gas-air mixture through the venting hole was considered. Overall, the ejection pressure was designed with a safety margin of 2.8 at the worst-case scenario, to ensure separation. More detailed information about the calculations can be found in ??.

#### First Deployment Design

To generate the required pressure without using large quantities of explosives, a CO<sub>2</sub> cartridge is pierced by a pin, which is accelerated using a small quantity of Nitrocellulose (NC) powder. The following figures show the different components (Figure 2.24) and how they are assembled (Figure 2.25).

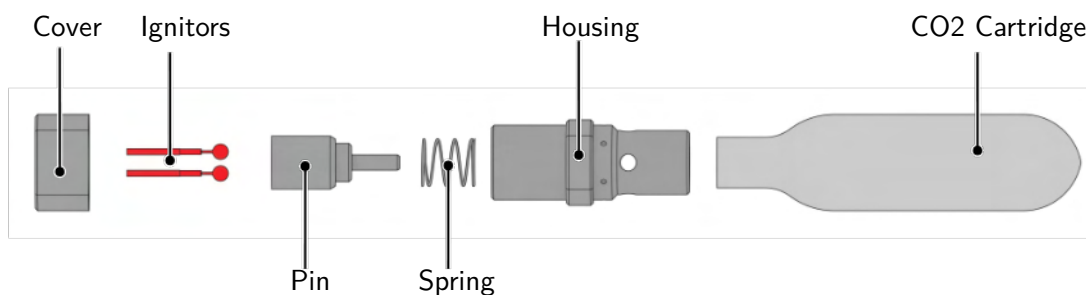


Figure 2.24: Exploded view of the first deployment components.

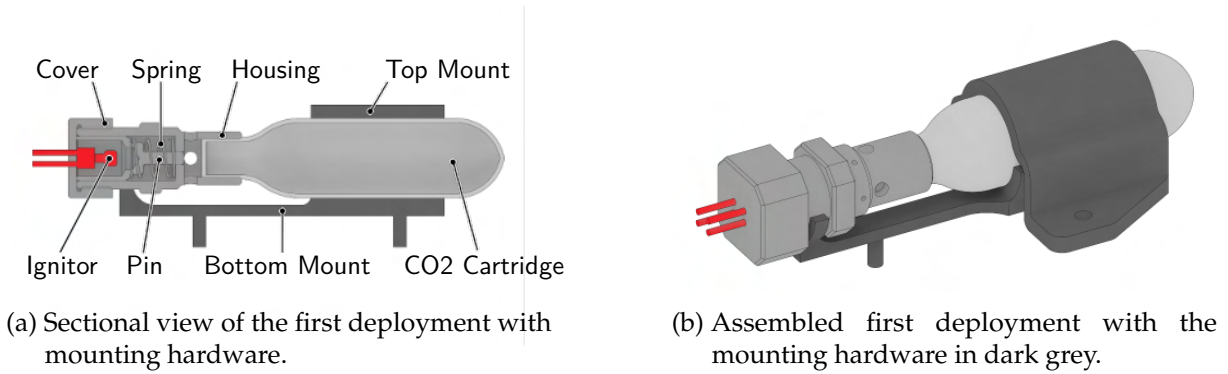


Figure 2.25: Detailed views of the assembled first deployment system.

**Pressure Chamber**

The pressure chamber is formed on one end by the payload retention plate inside the nose cone, on the other end, the pressure plate seals it from the rest of the rocket. Two first deployment cartridge systems are mounted together with the ignitor connection Printed Circuit Boards (PCBs) to the pressure plate, as shown in Figure 2.26a. Positioned in the center is the pressure plate connection bolt which connects the drogue to the rest of the rocket. The 3D-printed guide attached to the pressure plate prevents it from tilting during the extraction from the recovery tube. A sectional view can be seen in Figure 2.26b.

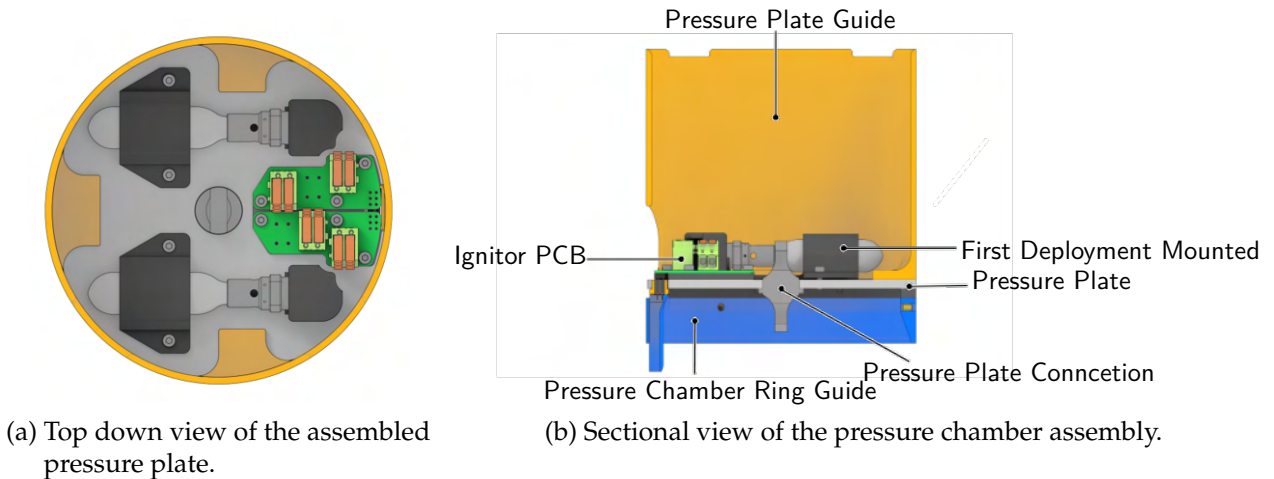


Figure 2.26: Detailed views of the assembled pressure plate and first deployment components.

**Explanation of the Mechanism**

The flight computers send their ignition signals to the PCBs inside the pressure chamber via wires running inside the cable duct (see Figure 2.26a). The ignitors, connected to the PCB, are triggered and ignite the NC powder. Expanding gas forces the opening pin into the CO<sub>2</sub> cartridge, piercing the membrane and releasing CO<sub>2</sub> gas into the pressure chamber. The high pressure shears off the pins holding the nosecone, ejecting it. The drogue is pulled out by the nosecone’s momentum, along with the pressure plate and main parachute bag.

**Redundancy**

Redundancy is achieved by using two identical first deployment cartridge systems. Each has two independent ignitors controlled by the two flight computers, as further detailed in Section 2.5.1.

If one of the two deployment systems fails and one of the two recovery electronics fails, the drogue parachute will still be deployed.

### Iterations

The design has been optimized for size and weight. CO<sub>2</sub> cartridges are smaller than argon ones, but still generate the required pressure. This size reduction allows the deployments to be mounted horizontally (as seen in Figure 2.26) instead of vertically, facilitating their placement directly in the pressure chamber.

### 2.4.2 Second Deployment

The objective of the second deployment is to initiate the deployment of the main parachute. The bag containing the main parachute is released during the first deployment but remains closed. This bag is referred to as a "free bag". At an altitude of 450 m above ground level, the connection to the main parachute is released by the second deployment mechanism, and subsequently, the bag can open. The main parachute is then suspended solely by the main shock cord, which tensions and absorbs the opening shock.

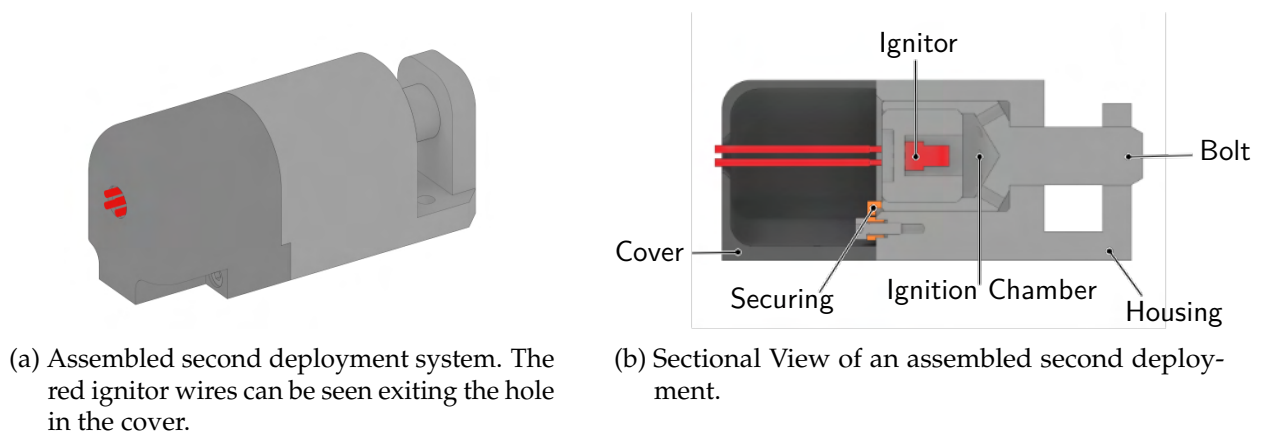


Figure 2.27: Detailed views of the assembled second deployment system.

### Design

The concept of the second deployment system drew inspiration from the tender descender mechanism. The primary objectives were to design the system compactly and firmly affix it to the groundplate.

As depicted in Figure 2.27b, the bolt is situated within the housing. The ignition of the NC powder generates an over-pressure, which accelerates the bolt, consequently releasing the rope that triggers the main parachute's opening sequence. To achieve a compact system, the ignition chamber was integrated within the bolt itself. Unlike the conventional practice observed in the tender descender, where the system is loosely tethered by two cords, the present system is secured to the groundplate's underside using screws. This fixed configuration was devised to mitigate potential issues arising from loose components within the rocket, which could lead to complications such as entangled ropes or rocket damage during different flight phases and landing.

Furthermore, to minimize heightened contamination, NC powder was employed instead of the commonly used black powder.

## Operating Procedure

The ignition of the NC powder takes place within the bolt's interior. The bolt is securely held in position by a 3D-printed retention device, the securing (see Figure 2.27b), which prevents premature bolt release. The ignition of the NC powder generates an over-pressure, accelerating the bolt and shearing off the retention device. This action detaches the second deployment line connected to the bolt, thereby releasing the link to the parachute bag.

To absorb the shock of the accelerated bolt and to keep it contained after deployment, a cover closes off the bolt's exit area. Several materials for the cover were tested: Polyamid 12/Nylon 12 (PA 12), Thermoplastic polyurethane (TPU), and even carbon fibre laminations. Ultimately, a moderately flexible TPU was determined to be the most effective at absorbing the energy.

## Redundancy

Redundancy within the system is ensured by incorporating two identical systems on the groundplate, as seen in Figure 2.28. Within each of these systems, two ignitors are installed. Notably, one ignitor can be activated by the COTS flight computer, while the other can be triggered by the SRAD flight computer.

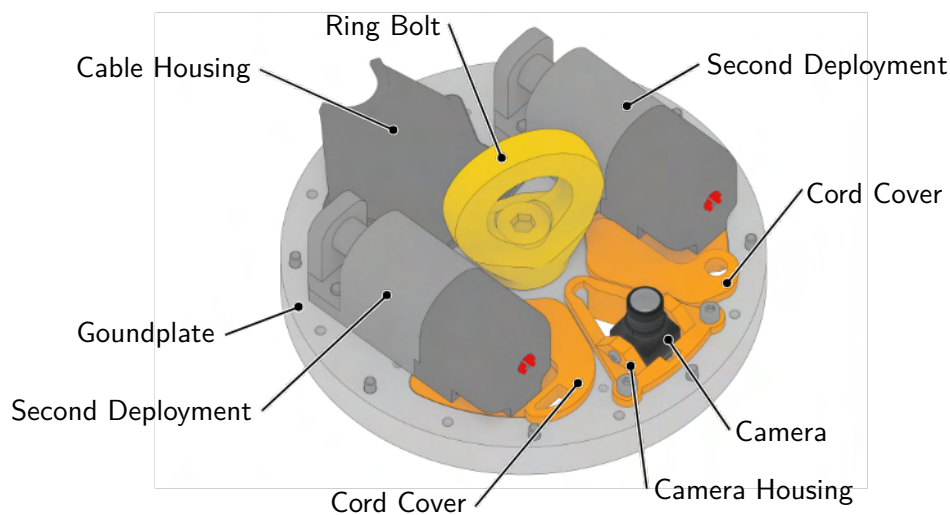


Figure 2.28: Fully assembled recovery groundplate.

## 2.4.3 Parachutes and Lines

### Parachute Design

The yellow drogue parachute has a cross-shape with a side length of 35 cm, as seen in Figure 2.29a. In a wind tunnel test where multiple different parachute shapes (taken from [3]) were evaluated, this shape was chosen due to its flight stability and drag benefits. The elliptical parachute prototypes oscillated and were unstable at the observed wind speeds. The lines are connected to the parachute by loops, as shown in Figure 2.29b. To reduce the force on the sharp bend, the loop material is used as a reinforcement by sewing it all the way to the other side, where the next ribbon ends in a loop. During measurements at various wind speeds (15, 20, 25, and 30 m/s), the average drag coefficient of the drogue chute was  $c_w = 3$ . With this value, a theoretical terminal velocity of 38.86 m/s is reached. The worst case scenario, regarding a premature deployment, was decided to be deployment into 100 m/s, where a shock force of 1417 N is expected (detailed information in the ??).



(a) Cross shape of the Drogue.



(b) Close up of a lash where the lines are connected.

Figure 2.29: Pictures showing the drogue parachute and its connection points.

The green and white elliptical main parachute has ten gores and twenty lines, symmetrically connected by V-shaped lashes, see Figure 2.30. The diameter is 3.2 m and the apex hole is 20% of the diameter, or 64 cm. Sensor data from the flight test showed a terminal velocity of 2.3 m/s, which yields a drag coefficient of  $c_w = 10.5$ . Due to the opening of the main parachute not being instant, a different approach for calculating the opening shock of 3.8 kN was taken. Further information can be found in ??.



(a) Elliptical shape of the Main Parachute.



(b) Close up of a lash where the lines are connected.

Figure 2.30: Pictures showing the main parachute and its connection points.

### Bag Design

The design of the parachute bag is inspired by commonly used rescue parachute bags for paragliding. The parachute bag has four leaves with a lug in the middle of each of them (Figure 2.31a). On one leaf, there is an elastic loop attached. This loop is threaded through the four lugs and afterwards the main shock cord is put through the loop to prevent it from slipping back out (Figure 2.31b). This means that the only way the bag can open is by putting the main

shock cord under tension, which is prevented until the second deployment event. During a drop test, the mechanism was tested with minimum weight to ensure the bag opens easily after the deployment. To confirm that the bag stays closed before the deployment, wind tunnel tests were performed. Additionally, the minimum drag force needed to extract the bag was determined.



(a) Parachute Bag Open.



(b) Parachute Bag Closed.

Figure 2.31: Graphical depiction of the main parachute bag.

### System Reliability Measures

To decrease the stress on all parts of the rocket during the deployment events, ductile shock cords with ultimate elongation of up to 27% were used. Additionally, a shock absorber to reduce the first deployment shock was implemented. An air-porous material was chosen to further decrease stresses on the parachute fabric, therefore reducing the shock force while increasing flight stability. To prevent rocket edges from damaging the shock cords during the descent, cord protections made of kevlar fabric were sewed onto the cords (Figure 2.32a). Furthermore, wherever ropes are attached to mechanical parts, thimbles, seen in Figure 2.32b, were added. The rotatable carabiner from Figure 2.32c will ensure that rotations on the rocket or the parachute will not be translated to the other part. In a wind tunnel test, the carabiner successfully decoupled the measurement device from the rapidly moving parachute even at 30 m/s.



(a) Rope protection sewed onto the shock cords.



(b) Thimble at the end of the connection lines.



(c) Rotatable Carabiner from the parachute lines.

Figure 2.32: Close-ups of thimble, rope protection, and the rotatable carabiner.

### Line Management

A visualization of the line management can be seen in Figure 2.33 and Figure 2.34. The actual line management during the main descent phase is shown in Figure 2.30a. During the drogue descent phase, the nosecone will be above the main rocket body since the pressure plate connection line I is longer than the nosecone connection line. During the main descent phase, the nosecone will

fly below the rocket body. The pressure plate connection lines I and II are combined 7 m long; therefore, the nosecone will not collide with the main rocket body.

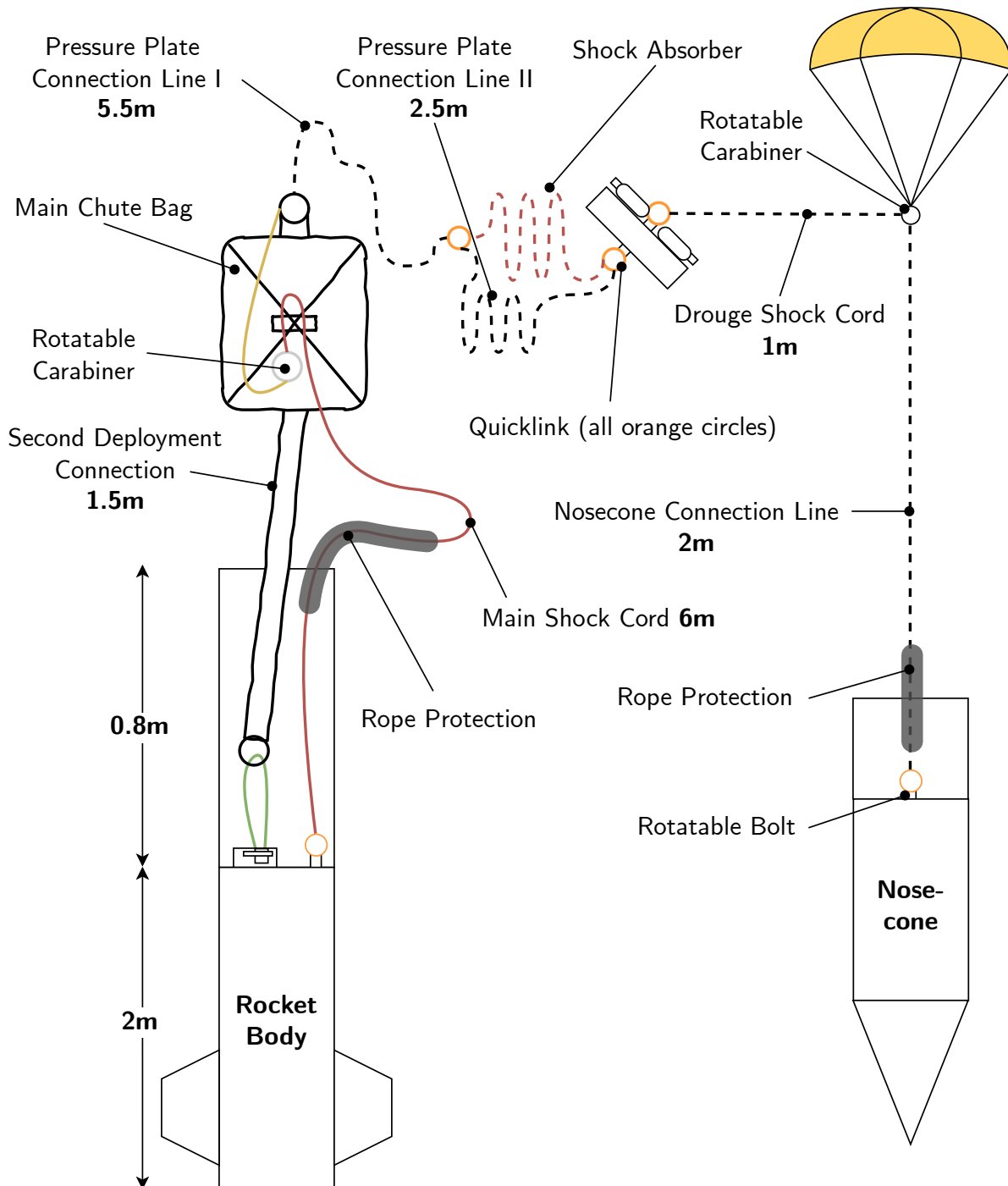


Figure 2.33: Line management after first deployment.

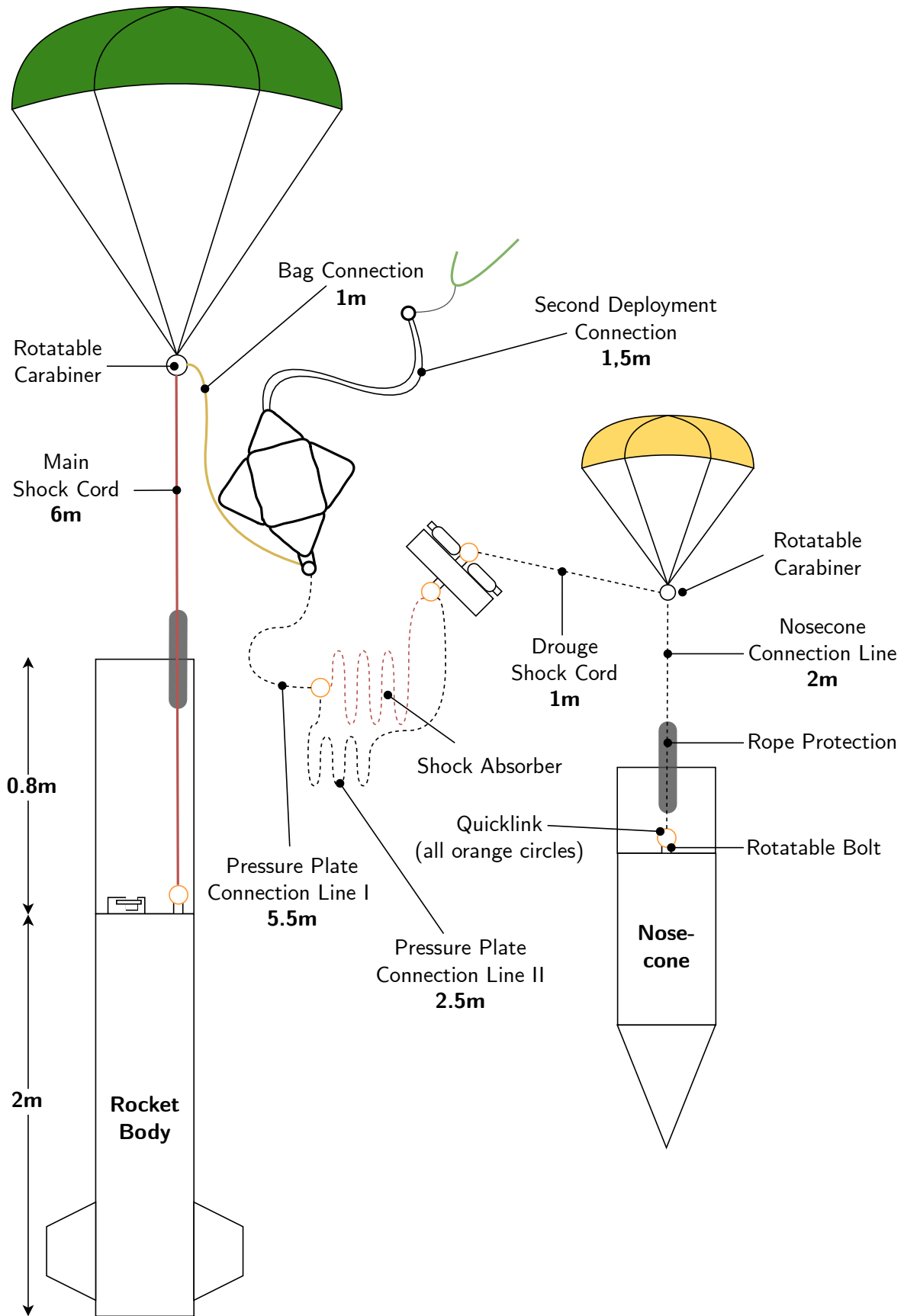


Figure 2.34: Line management after second deployment.

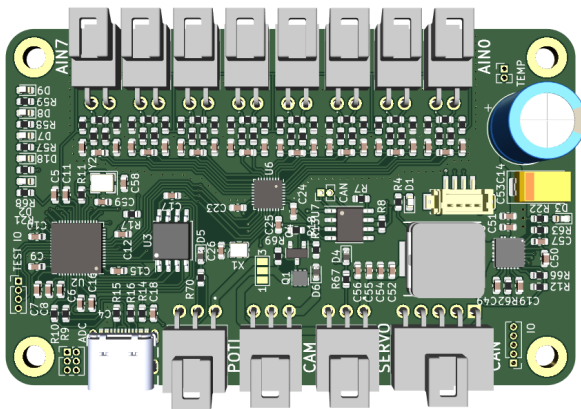


shown its ease of use and reliability in the previous project and was thus carried over with some minor form factor changes.

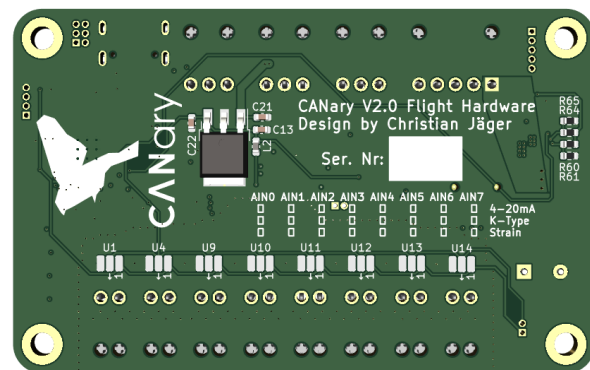
The recovery interface PCBs and first deployment PCBs serve only as passive interconnects for the recovery electronics. They route the different pyro-channels to lever-style terminal blocks for connecting the ignitor wires.

### 2.5.2 Sensor and Control Nodes CANary

The CANaries are SRAD PCBs that both sample sensors and control actuators while communicating with the FC via CAN Bus. The eight sensor channels can be configured individually for either thermocouples, pressure- or strain sensors. This approach allows maximum flexibility in later design decisions and a wide range of applications of the same hardware. In the same sense, a CAN Bus was chosen for virtually unlimited expansion potential. Each CANary has two actuator controls: a Pulse Width Modulation (PWM) servo output with an adjustable voltage supply and a high-power digital output.



(a) Front view with sensor connectors at the top and actuator and power connectors at the bottom.



(b) Back view of the CANary PCB.

Figure 2.36: Views of both sides of a fully equipped CANary PCB.

### 2.5.3 Power Management

The main power supply consists of a custom 7S (seven cells in series) Lithium Iron Phosphate ( $\text{LiFePO}_4$ ) battery module (shown on the right in Figure 2.37) with a capacity of 2500 mAh. This battery enables all rocket systems to run at full power for at least 3 h. To allow longer pad standby times, power is supplied over the electrical umbilical. The Backplane includes the circuitry to switch between power sources, either controlled by the FC or automatically in case the voltage of the active power supply drops below a threshold.

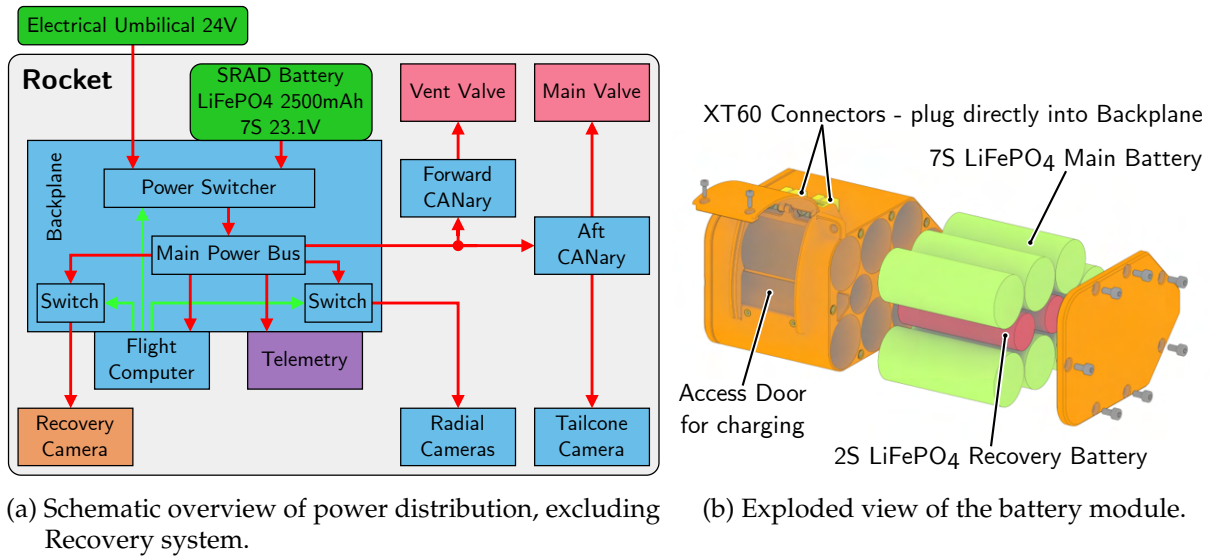


Figure 2.37: Rocket power system of the SRAD electronics.

### 2.5.4 Electronics Mount

The main objective of the electronics mount is to secure the PCBs, batteries, and cables in place during all times and still make it possible to quickly access all components until it is integrated inside the airframe. The Antenna Bay is attached to the bottom of the mount, and at the top of the mount is the connection to the REC-Groundplate. At the lower part of the mount, it is braced against the centering ring to prevent lateral movement.

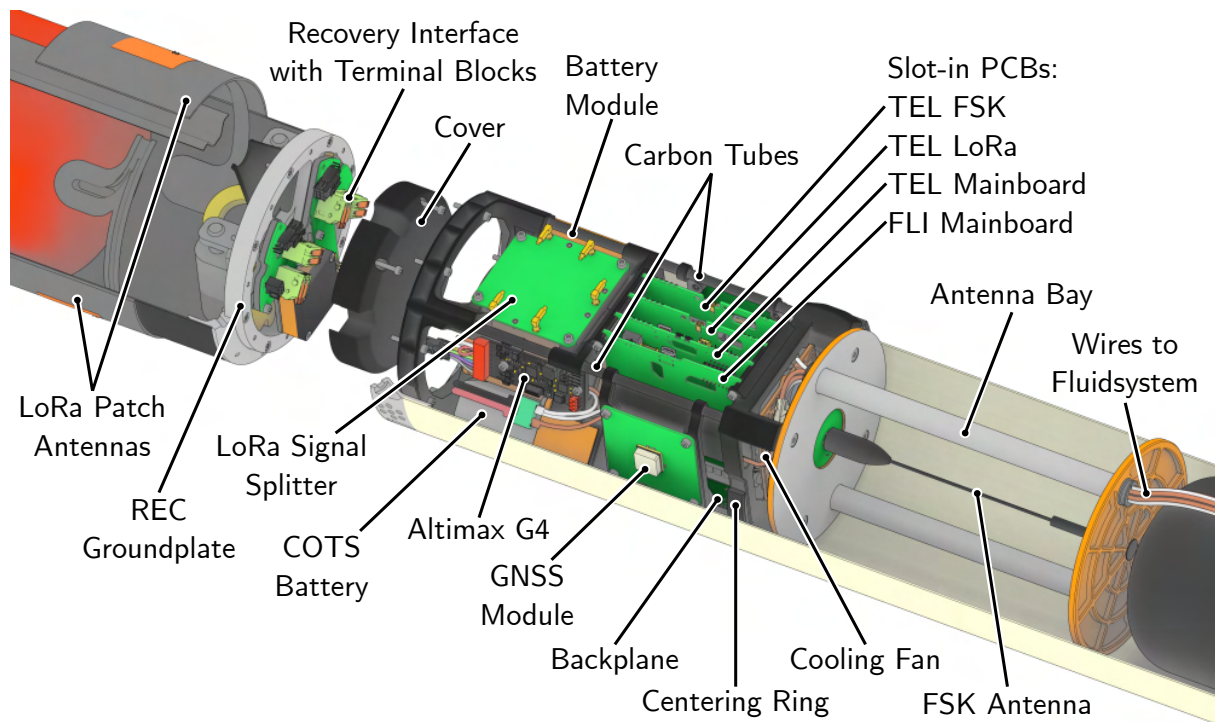
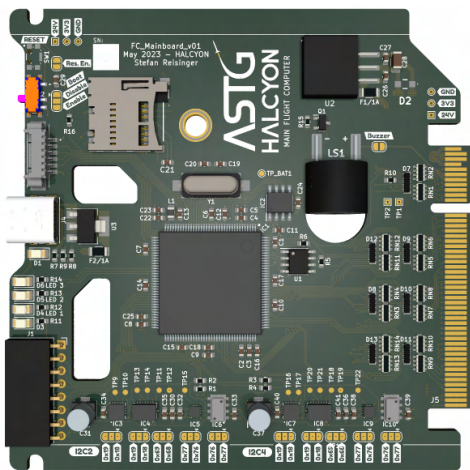


Figure 2.38: Overview of the electronics mount and all attached components.

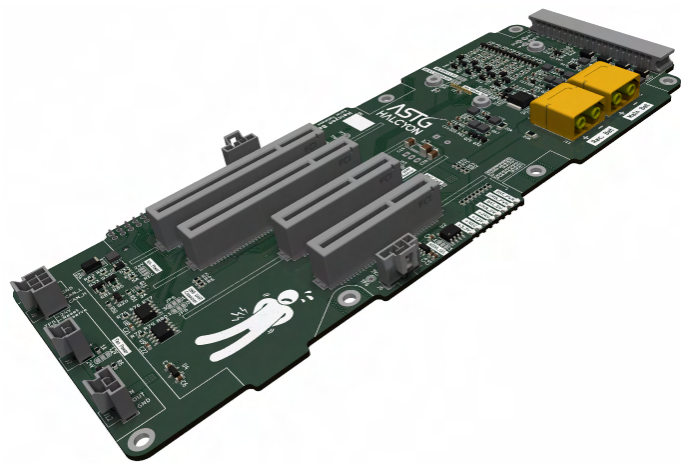
The mount itself is 3D-printed from Acrylnitril-Styrol-Acrylester (ASA), and the individual parts are joined by carbon tubes to ensure a stable connection and prevent the PCBs from being subjected to mechanical stresses. The 3D-printed parts are designed to allow airflow from a fan at the bottom to cool all components. Threaded inserts are embedded into the plastic to provide sturdy mounting points. One additional goal of the design was to ensure that only a small number of different tools are needed for the complete assembly of the electronics mount.

To keep all cables and connections to a minimum, the backplane PCB runs along the entire length of the electronics mount and serves as the central interconnect. The recovery interface at the top has a pin header that plugs into the backplane and provides a secure connection. The placement of the two GNSS-modules was designed to be at the outermost position possible to decrease "blind spots". The COTS FC is mounted to the side with its own battery and cables for arming and recovery deployment.

### 2.5.5 Mainboard and Backplane



(a) FC mainboard with microcontroller, sensors and onboard power supply.



(b) Backplane PCB of the electronics mount with PCIe connectors, battery sockets and various other connections.

Figure 2.39: FC Mainboard and Backplane PCBs.

### 2.5.6 State Diagram and Software

#### Operating System

The HALCYON FC software features an SRAD Real-Time Operating System (RTOS), called RavenOS, which is based on SmartOS[4] and tailored specifically to the use in projects of the ASTG. Using our own RTOS enables us to optimize for the chosen hardware and needed functionalities, significantly reducing code size and runtime overhead. As this year's software extensively uses external interrupts, RavenOS was updated to reduce the time needed to handle them. As the RTOS with the main software runs on the more powerful core of the STM32H745ZIT3 MCU, the second core can be used to offload time-consuming data management tasks.

#### Flight Computer Software

The FC software comprises tasks which concern themselves with one system functionality each. This allows for writing modular and well-structured code that can be reused in multiple projects.

This becomes evident when comparing the state diagram of the FC software of the rocket with the one of the Filling Station (FS), seen in Figure 2.40 and Figure 3.3, where some of the software states are virtually identical.

The different states the rocket's FC software can be in can be seen in Figure 2.40, split into green states, where the rocket is safe to handle and red states in which the rocket might be filled with fluids. On startup or after a reset, the FC gets initialized in the startup state. Everything in and around the rocket gets checked during the system check state. After this is done, the starting height and orientation are calibrated during the calibration state, after which the rocket enters the green idle state, where it waits for the FS to be ready for the Filling State.

During the filling and pre-launch state, the rocket and FS are synchronized, meaning they are always in the same state and can only advance to the next state together. If both FCs are ready for launch, the software can be advanced to the ignition state, where the rocket's FC waits for the ignition command sent by the Mission Control Box before initiating the countdown during which the rocket makes sure everything is ready for launch.

The countdown can be cancelled by flipping the two abort switches of the Mission Control Box simultaneously but keeping the FC in the Ignition State, ready to start the countdown again. If anything else unexpected should happen while the rocket is on the ground, the FC can be put into the soft abort state, where all actuators (except the engine ignitor) can be controlled by the MC to ensure the rocket can be put into a safe state.

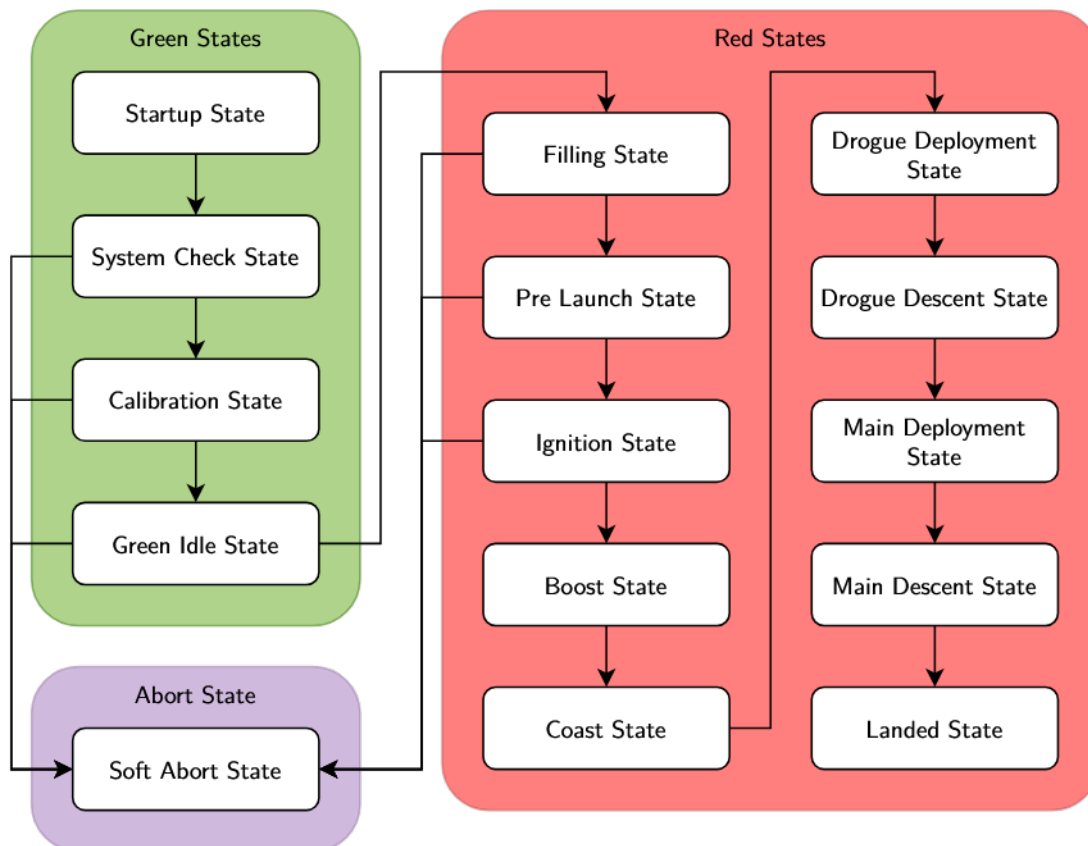


Figure 2.40: State diagram of the SRAD FC of the rocket, depicting the different states the FC software can be in.

If everything works as intended, and the rocket lifts off, the automatic state detection, described in Section 2.5.6, takes over and advances the rocket through the remaining states until it enters the landed state.

**Filter for Altitude Calculation**

To obtain the height value, barometer and Inertial Measurement Unit (IMU) data are fed into a Kalman filter. It provides sensor fusion as well as predictions in case of sensor failure. To account for the rocket’s orientation, the acceleration data is transformed from body coordinates into earth coordinates with the use of gyroscope data and quaternions. Following the application of the Kalman filter, the data undergoes additional refinement by utilising a moving average filter. This process aims to mitigate the impact of noise present in the output generated by the filter.

**Automatic State Detection**

The role of the automatic state detection is to transition from one state to the next during flight automatically. The diagram shown in Figure 2.41 illustrates all the states and the conditions that must be met to enter the subsequent state. Some states also have an additional minimum duration, which ensures that states are not prematurely skipped due to sensor noise during events like parachute deployment or engine ignition, as well as a maximum duration that prevents issues like frozen sensor data from preventing a state transition.

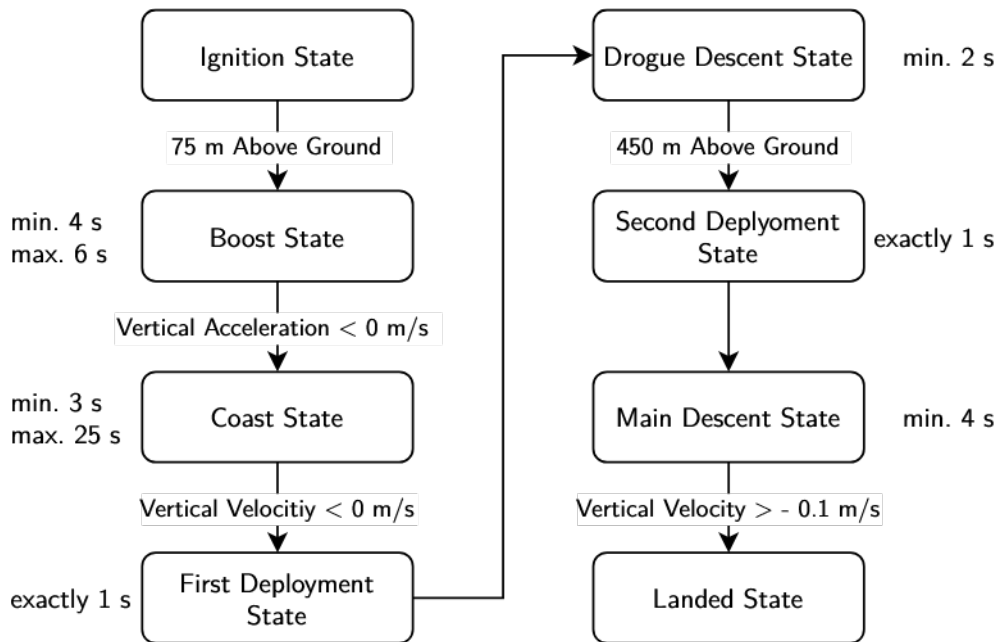


Figure 2.41: Automatic state detection used in the SRAD FC, showing the conditions needed for state transitions as well as the minimal and maximal times spent in some states.

**Actuator Safety**

To ensure all actuators are only actuated when they are supposed to, a check was included before each actuation to ensure the FC is in a state that allows the actuation. For example, the main valve can only be actuated during the system check state, ignition state, landed state, and soft abort state. The other safety-critical actuator, the engine ignitor, can only be actuated during the system check state and the ignition state. An extensive table listing all actuators and their respective states can be found in ??.

## 2.6 Telemetry Subsystem

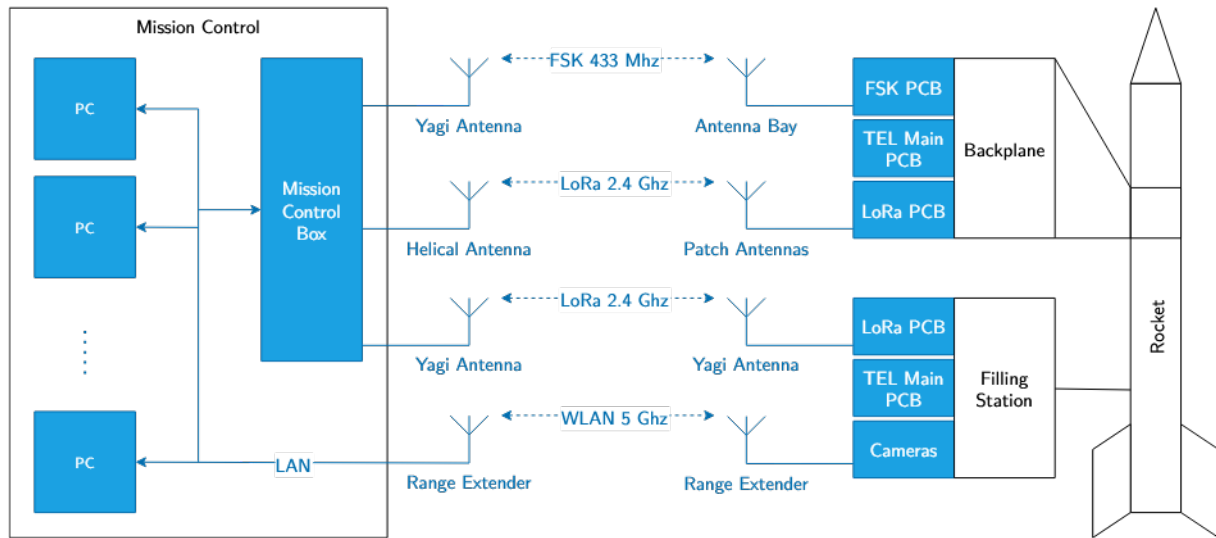


Figure 2.42: Overview of the whole TEL system.

The TEL main objective is to connect the rocket and the FS to the MC without any wires in order to control and monitor the status of all the system parts remotely.

To do this, we use two different types of Radio Frequency (RF)-links; one is based on the LoRa protocol, the other one over a simple Frequency-Shift Keying (FSK)-modulation. Both are used in the rocket while only LoRa is used in the FS. All parts use the same PCBs to make both design and programming easier. This approach followed from the past year's experience.

Over this simple connection, a network with its own package definition and routing follows, called ASTG Transport Protocol (ATP), and a Visualization with its accompanying backend.

### 2.6.1 Software

The three nodes of the TEL system (Rocket, FS, and Mission Control Box) operate using nearly identical firmware.

For optimal efficiency, both cores of our dual-core processor are utilized. One core is dedicated to data transmission, while the other handles data processing, routing, and tasks like reading data from the Global Positioning System (GPS) module and collecting hardware information. Communication with the FC occurs over a Universal Asynchronous Receiver Transmitter (UART) bus using Direct Memory Access (DMA), enabling efficient data exchange.

Another feature of our system is the emulation of full-duplex communication over our half-duplex communication links, achieved through the implementation of Time-Division Duplexing (TDD). This means specific timeslots are allocated for sending and receiving data on each link.

ATP is our solution for a low overhead protocol, which defines how MC, FC and FS communicate. It is implemented as a C library concerned with parsing and serializing ATP packets. This includes handling packet fragmentation, checking integrity with a Fletcher16 checksum, and collecting throughput/goodput statistics.

## 2.6.2 Visualization

The Mission Control user interface is a web-based software that runs on the MC server, located in the Mission Control Box. Multiple clients can connect to this server with a web browser via an ordinary Ethernet network.

Using this architecture has the benefit that operators/observers can bring their own Laptops and work independently.

Grafana is used for data visualization and a custom Vue.js app to execute commands. Those frontends are backed by a Python application and PostgreSQL. Everything is dockerized to ensure quick setup and reproducibility.

The Python application reads/writes ATP packets from/to a UART Universal Serial Bus (USB) device and stores the data in a PostgreSQL database. Most data is presented to the user with Grafana, which directly communicates with PostgreSQL. In order to execute commands, we developed a custom Vue.js frontend as a user interface, including some custom graphics to display the most important data. The Vue.js frontend communicates with the Python backend with a GraphQL Hypertext Transfer Protocol (HTTP) Application Programming Interface (API).

In addition to wired Ethernet in the Mission Control, we extend the network with a long-range WLAN solution to connect the four filling station IP cameras, which are used for visual confirmation.

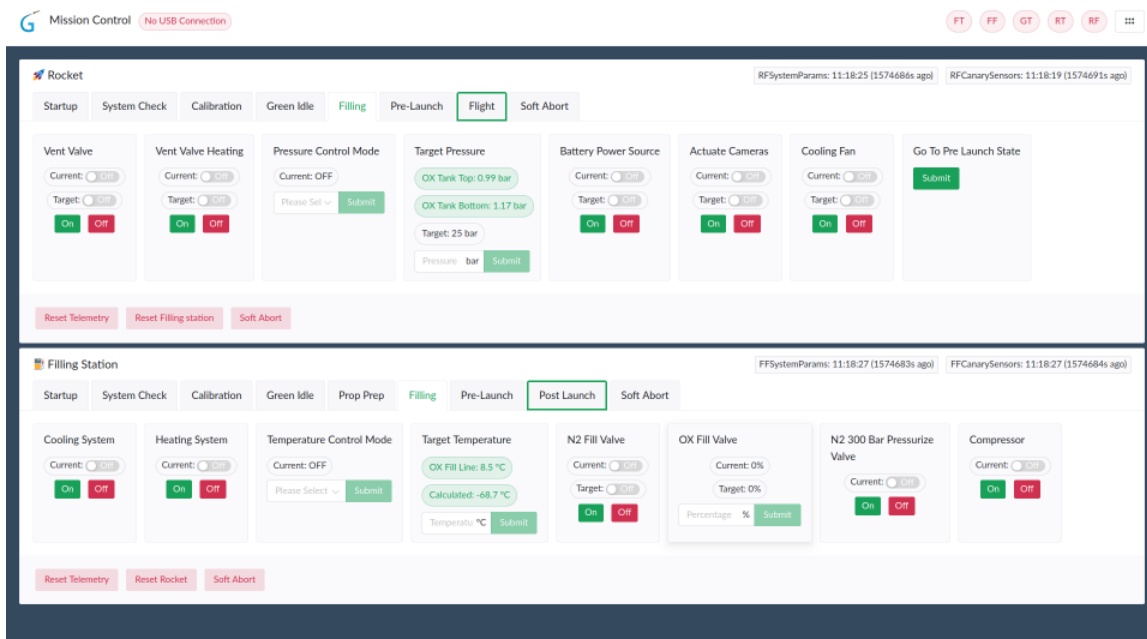


Figure 2.43: Screenshot of the Control Panel.

## 2.6.3 Hardware

The Telemetry hardware was designed using a modular approach. This enables the usage of the same PCBs in different combinations for all Telemetry nodes. To connect all the PCBs, Peripheral Component Interconnect Express (PCIe) connectors with a custom pinout and a Backplane PCB is used.

### Main Board

The main board is the centre of the Telemetry system. It contains the main processor, a RP2040, and the power supply for all Telemetry PCBs, consisting of three Direct Current (DC)-DC converters and a linear regulator. The first two supply power for the RF cards. The third DC-DC converter generates 3.3 V for all digital circuits in the whole Telemetry system, the linear regulator powers the analog subsystem, also with 3.3 V. The analog subsystem contains an Analog-to-Digital Converter (ADC) and two multiplexers. It enables the main board to measure different voltages and currents on it and the RF cards.



Figure 2.44: Main board.

### FSK Board

The FSK board is used for communication between the rocket and the Ground Station (GS). It operates in the 70 cm amateur radio band, with up to 38 dBm of output power. To generate and receive packets, the Silicon Labs Si4463 transceiver Integrated Circuit (IC) is used. Two-way communication is enabled by using an RF switch. A low-pass filter near the RF connector prevents harmonics from being transmitted.

To prevent overheating of the Power Amplifier (PA), an aluminium heat sink and a small radial fan are connected to the bottom side of the board.

The RF section of the board is covered by a custom-made metal shield to increase the attenuation of unwanted signals and to decrease unwanted radiation.

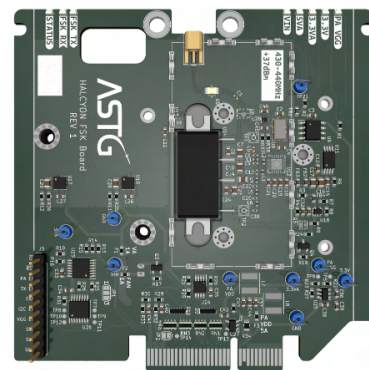


Figure 2.45: FSK board.

### LoRa Board

The LoRa board is used for all telemetry links in the system. Depending on the power level set and the local regulations, it can operate in the 2.4 GHz amateur radio band or the wireless band for Industrial, Scientific, and Medical purposes (ISM) band. It uses the Semtech SX1280 LoRa transceiver IC in combination with a Skyworks FEM with up to 30 dBm output power and an integrated RF switch and Low Noise Amplifier (LNA), enabling two-way communication.

A small heat sink is attached to the backside of the board to prevent overheating during high ambient temperatures.

On the top side of the board, a custom metal shield covers the RF section to improve performance, similar to the FSK board.

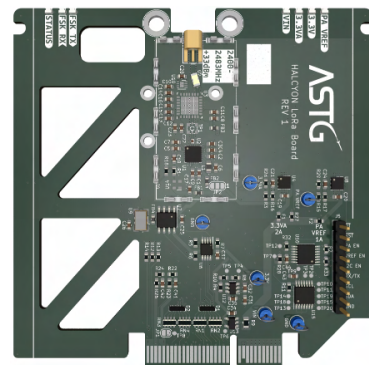


Figure 2.46: LoRa board.

### GS Backplane

The GS Backplane is used in the Mission Control Box, in combination with a 3D printed part, to securely hold the PCBs and connect them electrically.

It contains a power input with protection circuits, seven digital inputs for switches, and eight digital outputs to control 24 V LEDs.

The connector used to interface the main board with MC server, with the help of a USB-UART adapter, is also located on this board.



Figure 2.47: GS Backplane.

## 2.6.4 Antennas

We decided to use two antennas for the two frequency links as combining them into a multi-band antenna proved impractical.

### Antenna Bay

For the FSK link (430 MHz / 70 cm band), a  $\lambda/4$  monopole antenna with a ground plane was used since the ground plane should be relatively large compared to the wavelength, the maximum diameter (circumference of the rocket) was used. Some 12 mm cable channels were introduced, as visible in Figure 2.48. These influence the wave impedance of the monopole, which then was matched with an L-matching network. The whole structure was simulated in CST Microwave Studio.

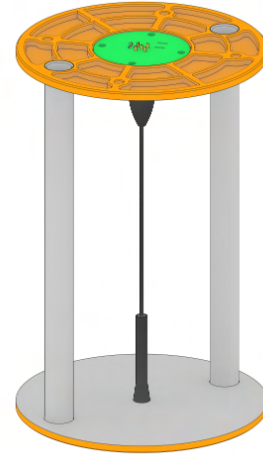


Figure 2.48: FSK Antenna Bay.

### Patch Antennas

The LoRa link (2430 MHz / 12.5 cm band) uses patch antennas, which are quite well suited for our application. They can be mounted on the outside of the rocket, which saves space, and because of their functional principle, anything can be mounted behind them without interfering.

Since an omnidirectional radiation pattern is desired, we settled on four patches circularly around the rocket. They are all connected with a 1-to-4 Wilson power divider, which we also designed.

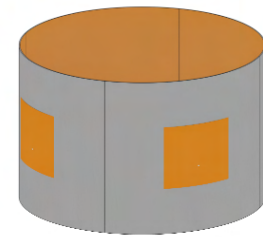


Figure 2.49: Patch antenna ring.

## 2.7 Payload Subsystem

HALCYON is designed to carry a payload of 3 x 1U CubeSats with a total mass of almost 4 kg in the NC-S (more details in Section 2.3.3) to the target altitude of 3000 m. Like previous projects, this year's payload consists of two projects built by students from Polytechnic High Schools and one project as part of the Bachelor thesis of a team member. All three Projects use the ASTG designed CubeSat structure. Each project team compiled a more detailed payload description, which can be found in the ??.

### 2.7.1 CubeSat Colibri

Colibri is the name of the CubeSat developed for a Bachelor thesis. The idea behind this project is the development of a camera system to get clear and steady video footage during and after the drogue deployment and until touchdown. Since the nose cone can spin freely around the ropes of the chute, the challenge was to stabilize the camera along the vertical axis like a gimbal. To achieve this, a servomotor can move the camera and its PCB in any desired position. Furthermore, a BMI088 IMU is used to measure gyro and accelerometer data, which are then used by a ESP32 MC to give the position signals to the servo controller (TMC4671). The system is powered by four serially connected 18650 Lithium-Ion (Li-Ion) cells.



Figure 2.50: CAD of CubeSat Colibri.

### 2.7.2 CubeSat PATHOA

PATHOA stands for "Pressure, Acceleration, Temperature, Humidity, Orientation, Altitude" and describes the functionality of this student-built CubeSat. The team from HTL Kaindorf used a Raspberry Pi Pico, which they programmed using Python. With the included Bosch Sensortec BME 680, the CubeSat can measure temperature, humidity and pressure, and using an MPU 6050, it can sense acceleration and orientation. Everything is powered by two 18650 Li-Ion cells. Also on board is the first ASTG astronaut in the form of a toy figure.

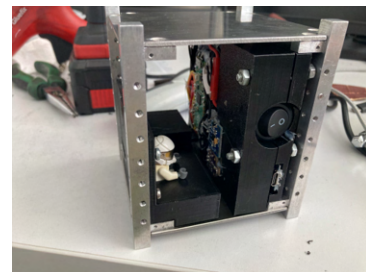


Figure 2.51: Foto of CubeSat PATHOA.

### 2.7.3 HPD's CubeSat

HPD, or Halcyon Payload Development, is a team of four students from HTL Pinkafeld. They designed and developed a CubeSat to measure the muons in cosmic radiation during the rocket's flight. Afterwards, the collected data will be visualized. To achieve their goal, the students used a Raspberry Pi 3B with a custom plug-on board by MuonPI, which is responsible for measuring the muons and the corresponding timestamps. The MuonPI has an integrated silicon photo-multiplier to detect the light emitted by a plastic scintillator if excited by a muon. The measurement unit is powered by Samsung INR18650-30 Li-Ion power cells.



## 3 Ground Support Equipment System Architecture

### 3.1 Filling Station

The Filling Station (FS) consists of 3 major parts: the filling panel with the actuators and measuring equipment of the fluids, the Oxidizer bottle holder and the main electronics cabinet.

#### 3.1.1 Fluid Architecture

The filling panel consists of two fill lines. One for the  $N_2O$  and the other one for the pressurizing gas. They are connected on one side to the fluid bottles and on the other to the umbilical connection. In the  $N_2O$  line, the fill valve is an adapted version of the servo-actuated main valve from the rocket. For monitoring the state of the  $N_2O$ , an opened bottle valve is mandatory. To ensure no single point failure when the  $N_2O$  bottle is open, thereby endangering the personnel next to the filling station, a manual fill valve was added in series. For the pressurizing line, the goal was to be as independent of the available consumables as possible. For this, the line has three possible inlets, two of which are for  $N_2$  bottles and one for a high-pressure compressor. All other valves on the filling panels are solenoid valves because they are simple to actuate and show high reliability. For monitoring the pressures and temperatures in the filling panel, several sensors are added to the fluid system, as can be seen in Figure 3.1.

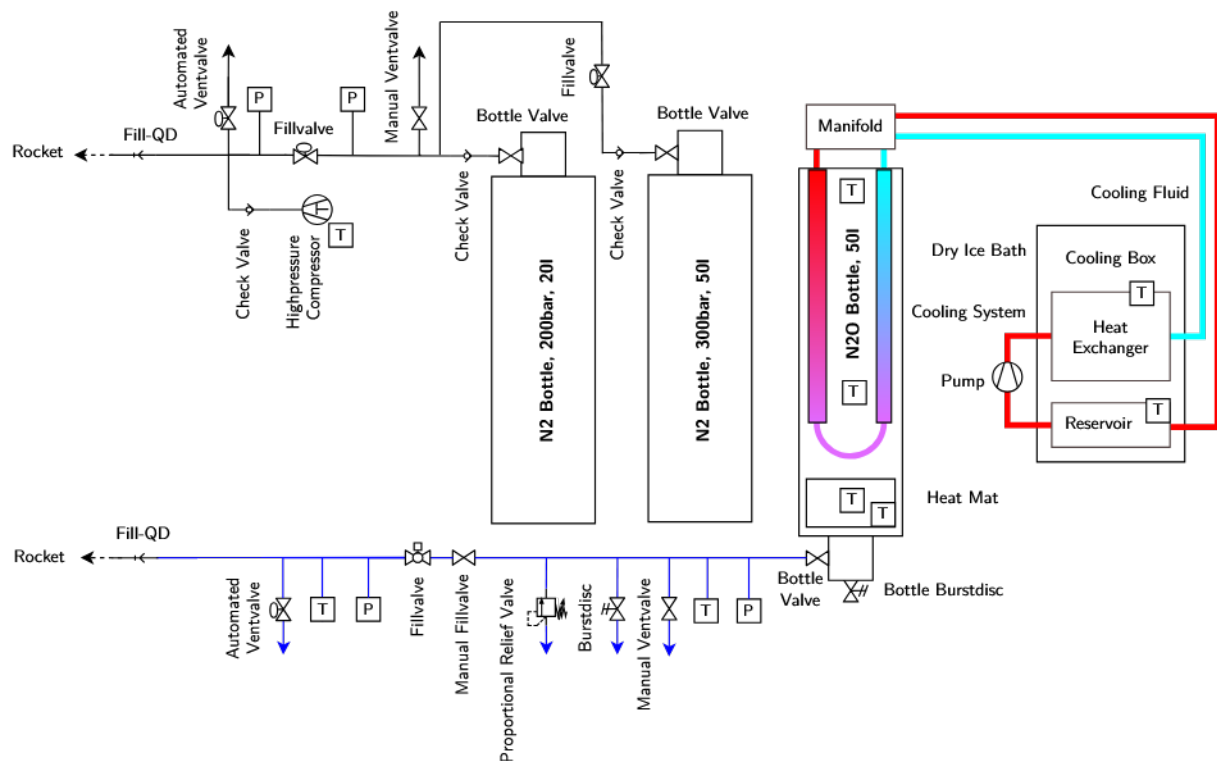


Figure 3.1: Fluid system schematic of the FS.

### 3.1.2 Electronics Architecture

The FS uses a 400 V/16 A main power supply and a 24 V/6 A control electronics supply. Sensor readout and actuator control are done via CANaries connected to a flight computer mounted inside the electrical cabinet, which has its own telemetry link to MC. Using the same hardware as in the rocket enables the reuse of large parts of the code base and decreases the time needed to develop and test additional PCBs. On the cabinet door, multiple lamps show the system’s current status. Additional switches and buttons allow manual overrides for important functions (e.g. vent valves, cooling pump, and FC reset).

Due to Electro Magnetic Interference (EMI) problems experienced during testing, the readout of sensors is separated as much as possible from high-power actuators. This is done by separating the CANaries in their own electrical cabinets and keeping the sensor cables as short as possible and shielded. The main power consumers (e.g., the cooling pump and compressor) are also connected to different phases than the control circuitry.

### 3.1.3 Safety Precautions

To protect against electrical shock and equipment damage, the FS implements several safety devices: Main load break switch, overload fuses, Residual Current Device (RCD), and circuit breakers. Additionally, emergency stop switches at the FS and the safety control box can disable all high-power devices while keeping the control circuitry powered on. Together with the 24 V lead acid backup battery, this ensures the continued readout of all sensors to keep track of the fluid system state and prevents potentially dangerous states from going unnoticed.

To increase the safety of the fluid handling, several components were implemented. Mainly, as already mentioned in Section 3.1.1, the manual fill valve was added. In addition to that, a burst disc and a proportional relief valve were also included between the N<sub>2</sub>O bottle and the manual fill valve. Furthermore, manual vent valves are included in both lines to secure the filling station after a launch or electronics failure.

The path of the ignition signal is shown in Figure 3.2. The reason why it originates from within the rocket is to have precise timing between ignition and main valve opening. The safety control box, which is located more than 15 m away from the launch rail, enables the automatic control of valves, houses the safety interlock for the engine ignition, and provides the connection for the ignitor wires.

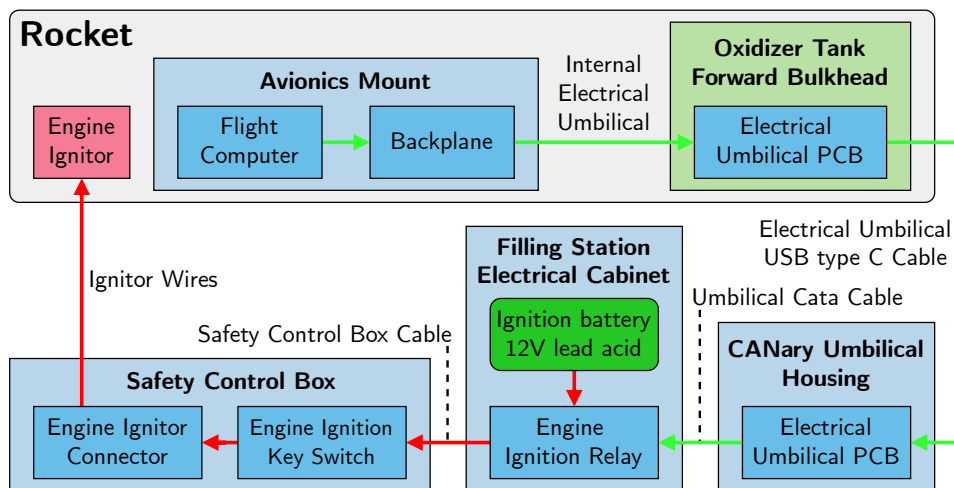


Figure 3.2: Schematic diagram of ignition electronics.

### 3.1.4 State Diagram and Software

As already mentioned in Section 2.5.6, the FS uses the same RTOS and general software structure as the rocket's FC. This goes as far as using the same code, with slight adaptations for the four green states. The most notable difference is the addition of a yellow state, the Propellant Preparation State. In this state, the FS is still independent of the rocket and can start to prepare the fluids for tanking. For this, some of the bottles might already be opened, which results in only specialist personnel being allowed near the FS. After the rocket has arrived at the launch rail, the rocket can command the FS to advance to the Filling State and further to the pre-launch state. When the rocket FC gets the ignition command and enters the countdown, the FS advances to the Post Launch State, where all valves can be actuated to bring the FS into a safe state after launch. The FS features the same Soft Abort State as the rocket, which can be triggered by pressing a button in the MC software. In this state, everything can be actuated to react to every possible situation.

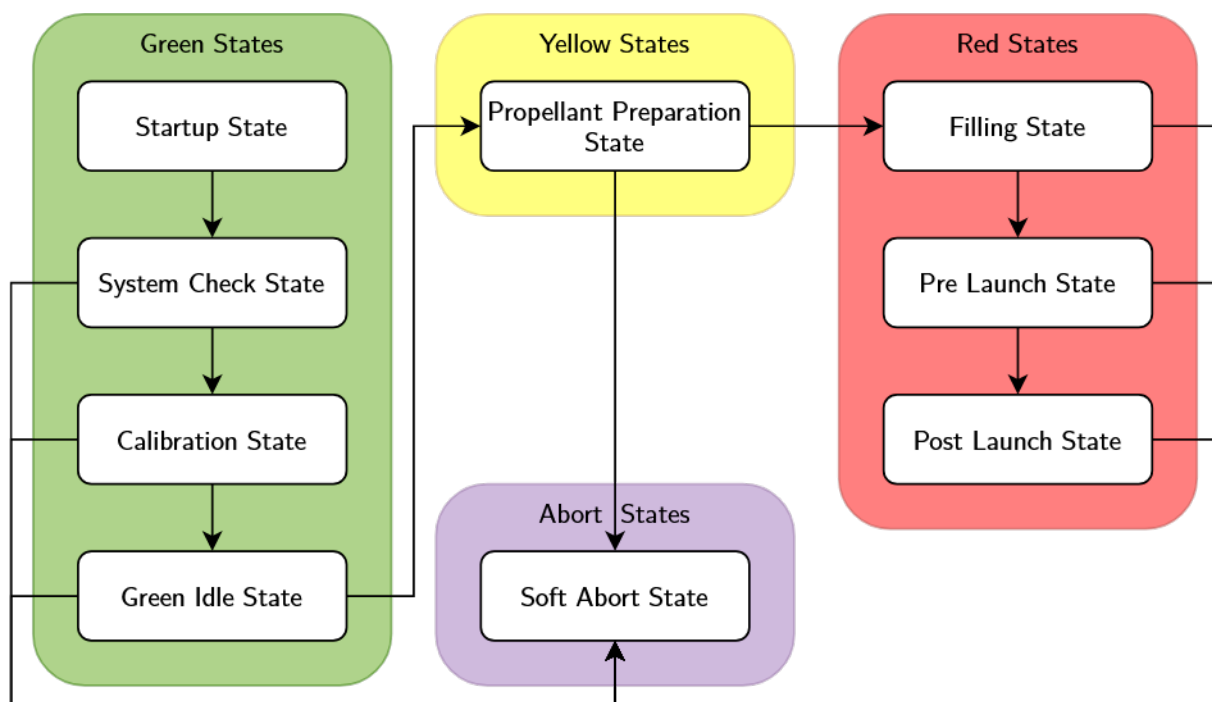


Figure 3.3: State diagram of the FS, depicting the different states the software can be in.

Regarding actuator safety, the FS features the same implementation as the rocket software, described in Section 2.5.6. The table listing all actuators and states of the FS can be found in ??.

## 3.2 Umbilical Connections

### 3.2.1 Fluid Umbilicals

The primary role of the fluid umbilical is to detach the rocket from the filling station after the fueling process is completed. This separation is carried out by first releasing the two Quick Disconnects (QDs) connections and then swinging the whole arm back by 180° to get it out of the way of the exhaust stream during launch.

The release of the oxidizer and pressurant QDs works as follows: A servo motor pulls back on the actuation sleeve of the female side of the QD. At the same time, the assembly is spring-loaded against the rocket's hull to increase the force with which the QD coupling is pulled out. This additional spring loading was added after first tests showed that the built-in springs of the QD couplings are not strong enough for reliable disconnects. In order to allow for a manual release, the connections from the servo motors are not rigid and instead use steel cables. This way, the couplings can also be opened by pulling on the clearly marked handles.

To swing the arm back by 180°, the rotational joint is preloaded using springs. In order to still be able to actuate it by using a servo motor, a mechanism similar to a mousetrap was designed. The motor pulls back on a PA 12 3D-printed bracket, which hooks onto an aluminium snap hook mounted to the pivoting part of the arm. To ensure a successful release, the position of the arm is monitored using a potentiometer.

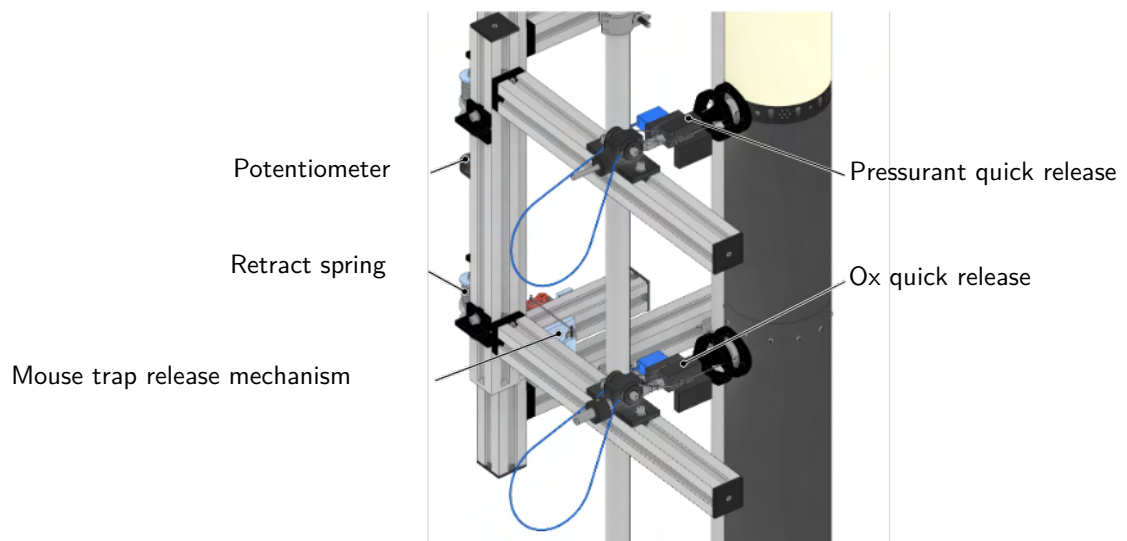


Figure 3.4: Umbilical arm with quick disconnects

### 3.2.2 Electrical Umbilical

The electrical umbilical functions as a wired connection between the rocket and the GSE while the rocket is on the launch rail. It utilizes a Type-C USB cable due to its compact connectors, high power rating of 240 W, and high data transfer speed of up to 40 Gb/s. The connector on the launch vehicle is situated at the top of the oxidizer tank, angled downwards to allow unplugging during the acceleration phase along the launch rail.

One main function of the umbilical is the auxiliary power supplied to the rocket to keep the onboard battery pack charged until lift-off. Besides power delivery, several other important signals are carried over the cable: the ignition signal, an ignition echo to confirm the switching of the contactor, two-way reset signals, and a serial data connection in case of telemetry problems. The reset lines can be used to remotely reset the rocket using the FS and vice versa.

On the other side, the electrical umbilical connects to a small electrical cabinet mounted to the back of the launch rail. The cabinet also houses three CANaries, which control the fluid umbilical servos and read the sensor data of the wind speed sensor and the rocket weight measurement system.

### 3.3 Temperature Condition System

To achieve high fluid density in the  $N_2O$  tank, a cooling system is essential. This cooling system consists of cooling jackets that are fastened onto the  $N_2O$  bottle, along with two heat exchangers, a pump and a reservoir. The two connected heat exchangers are placed in a plastic tub, which is then positioned within an insulated wooden box. On top of this box, the pump and reservoir are placed. This design allows for a compact structure known as the cooling box. The heat exchanger outlet is connected to the cooling jackets through insulated tubing, and the flow is subsequently returned to the reservoir. The cooling jackets are constructed using copper tubes pressed into copper plates, which are curved around the bottle. Two jackets, each with four tubes pressed into them, are connected in series. To distribute the flow, manifolds are utilized and linked by quick couplings to the insulated tubing. Dry ice is used as a coolant, achieving temperatures as low as  $-60\text{ }^\circ\text{C}$  in the dry ice bath. The cooling cycle is filled with approximately 17 L of isopropanol with additional 50 L in the dry ice bath, covering both heat exchangers. Isopropanol was chosen as a cooling fluid, as it remains sufficiently liquid at these low temperatures. The heat exchangers are necessary because pumping the dry ice-cooled isopropanol directly causes outgassing, making pumping impossible.

In the tanking process, further detailed in Appendix B.2.3, it is necessary to heat the  $N_2O$  bottle to increase the pressure in the oxidizer system. This is needed to create a pressure differential to enable subsequent venting of the oxidizer tank. This results in liquid  $N_2O$  flowing from the ox bottle to the oxidizer tank as the pressure equalizes. For this purpose, a 600 W heating mat is attached to a curved copper plate, which is then fastened onto the bottom of the  $N_2O$  bottle.

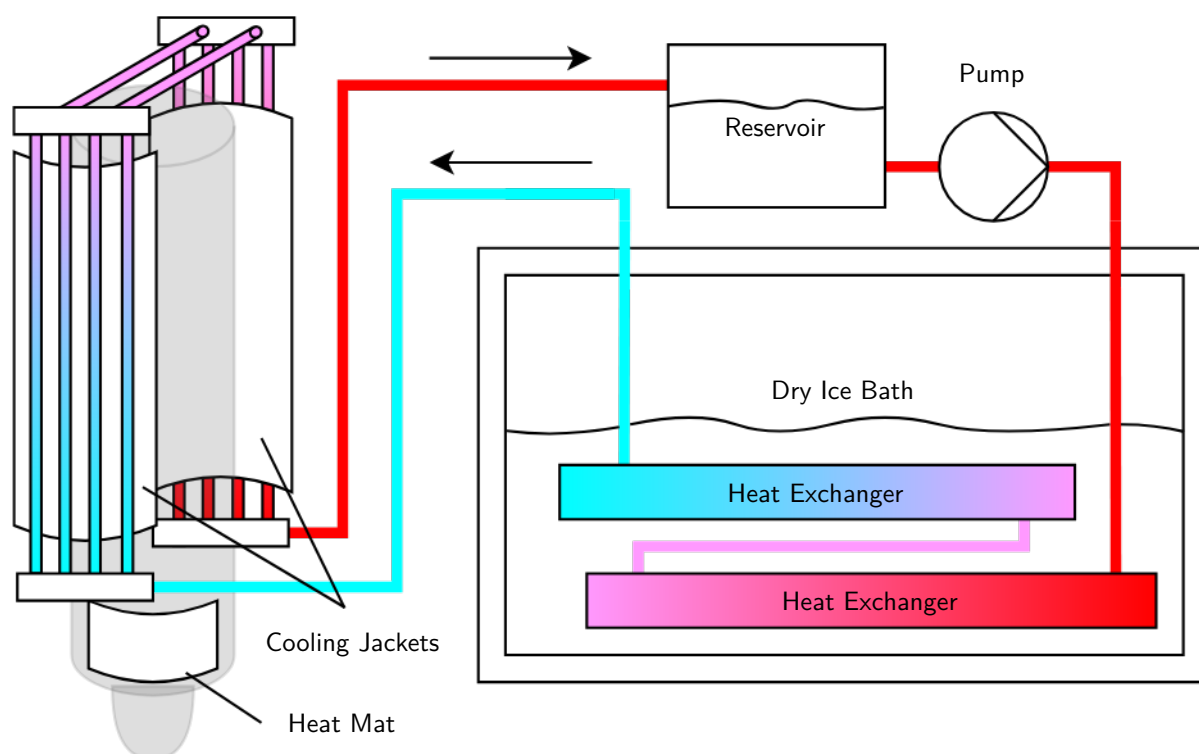


Figure 3.5: Schematic of the cooling cycle depicting the cooling jacket and heat mat around the  $N_2O$  bottle on the left and the cooling box on the right side.

## 3.4 Mission Control

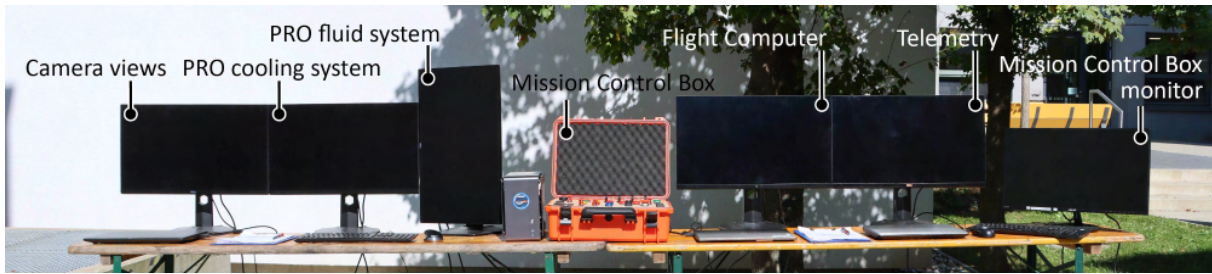


Figure 3.6: MC setup, antennas are not visible.

The MC consists of hardware and software, which is used to control the FS and rocket from a safe distance. For this, two RF-links to the rocket and one to the FS are implemented. The TEL hardware is housed in the Mission Control Box, which also serves as a physical interface for its users. All other information and controls are then visualised on multiple monitors connected to Personal Computers (PCs) over an ethernet connection.

The typical configuration of the Mission Control can be seen in Figure 3.6 with all the monitors and their dashboards functions. The protocol writer would then sit in a second row with other experts to advise the MCs operators.

### 3.4.1 Mission Control Box

The Mission Control Box houses all of the TELs electronics on the ground and provides a physical interface to control the flight and its preparation. It houses the server, where the visualization and its backend run, all necessary PCBs and electronics to support them. The orange case, as seen in Figure 3.6, was chosen to make it easy to move and set up the TEL system while giving it more resilience against external factors.

### 3.4.2 Antennas

Two of the three wireless links from the MC utilize regular Yagi antennas. These are the LoRa link to the FS and the FSK link to the rocket. Both of them are mounted stationary on a tripod.

For the LoRa link to the rocket, a helical antenna was built and will be tracking the rocket manually during the flight. This was done with the fact in mind that if the rocket comes into a horizontal position, the polarization of an ordinary antenna will be crosswise to the rocket's Antenna Bay, and therefore no signal will be received. By using a helical antenna, the polarization is rotating, which means that we will get a slightly worse signal (-3db) all the time, but we will never lose contact.

## 4 Mission Concept of Operations Overview

To successfully and safely fly and land HALCYON, a detailed mission concept was developed. It includes the preparation of the rocket on the launch day, setup of the MC as well as the FS and, if applicable, the launch rail. It is split into three main phases: the pre-flight handling and tanking phase, the flight itself, and the post-flight phase.

Table 4.1: Tabulated concept of operations.

Mission/ Operational Phase	appr. Time (start)	Phase End	Assembly Tent Team		Mission Control Team		Launch Rail Team		Recovery Team
Storage & Transport	T-7d	Arrival at the launch site	Parts are stored in boxes  The propulsion stack is preassembled with the ignitor installed and shunted  The avionic bay is preassembled		The mission control is stored in boxes		The launch rail is disassembled (if applicable)  The cooling fluid (isopropanol) is stored in canisters  The dry ice is stored in Styrofoam boxes		
Pre - flight - handling	Assembly	T-3h  The rocket is assembled and brought to the launch rail	Assembly of the recovery subsystem		Setup of the mission control		Setup the launch rail (if applicable)		
			Assembly of the avionics subsystem		Establish connection with the filling station and its cameras		Setup the filling station with its antenna system		
			Visual inspection of the preassembled propulsion stack		Establish connection with the rocket for last checks		Setup the cooling loop		
			Final test actuation of the flight hardware		Report first sensor data of the filling station		Install the N2O and N2 Bottles		
			Payloads are switched on				Purge the filling system		
			Integration of all Subsystems into the Rocket				Pre-chill the N2O Bottle		
	T-1h	The specialist personell leaves the launch pad			Final checks of the filling station		Mount rocket to the launch rail  Connect umbilical  Final checks of the filling station		Prepares for the recovery of the rocket
							Arm rocket, open manual N2O valve and connect ignition		
Tanking	T-30 min	The rocket is fully tanked, pressurised and the umbilical disconnected			Controlling the tanking circle  Final go/no go round for launch  Remote disconnecting of umbilical		Stay alert in case of an abort  Possibility of manual umbilical disconnect		
			Payload	Aerostructure	Flight computer	Telemetry	Propulsion	Recovery	
Ignition	T-1s	The ignitor is burning			Transmits the signal through the electrical umbilical to the filling station	Receives the ignition signal and hands it to the flight computer	Ignitor is ignited		

				Payload	Aerostructure	Flight computer	Telemetry	Propulsion	Recovery	
Flight general	Lift - Off	T = 0s	The rocket starts moving under its own thrust		Rail buttons provide stabilisation on the launch rail	Open the main valve	Rocket communication and data downlink	Booster fires after the main valve is opened		
	Power Ascent	T+0s	The rocket is not accelerating upwards anymore	Records flight data		Measure flight parameter	Relay propulsion system data + rocket data			
	Coast Phase	T+6s	Apogee is detected by the flight computers			Measure flight parameter	Transmit rocket data			
	Drogue Deployment	T+27s	Drogue is deployed	Films the drogue deployment for post launch analysis		Ignite the drogue deployment	Confirm drogue deployment via datalink		The gas capsules of the drogue deployment get punctured and pops off the nosecone	
	Drogue Descent	T+29s	Reaching an altitude of 450 m	Measurement of cosmic radiation		Measure flight parameter	Transmit rocket data		The drogue chute slows the rocket to 38.8 m/s	
	Main Deployment	T+139s	The main parachute is fully deployed			Triggers the main deployment at 450 m	Transmit rocket data		The pyrotechnic charge opens the tender descenders, releasing the main parachute	
	Main Descent	T+141s	The rocket touches down			Measure flight parameter	Transmit rocket data		The main chute slows the rocket to 2.3 m/s	
	Landing	T+210s	The area is free for recovery operations				Transmits the GNSS position of the rocket			
				Assembly Tent Team		Mission Control Team		Launch Rail Team		
Post flight	Recovery	T+30 min	The rocket is brought into the assembly tent	Prepares to receive the rocket for final disassembly		Leads the recovery team with GNSS data Actuates the valves on the filling station to depressurise system		Closing of the gas bottles Depressurisation of the filling station		Recovery of the rocket
	Disassembly	T+1h	The rocket, filling station and all tools are stored	Disassembly of the rocket Stowing of the rocket		Saving of all data First analysis of the data and final flight height Take down of the mission control		Disassembly of the launch rail (if applicable) Filling the isopropanol into canisters Disassembly of the filling and cooling station		

### 4.1 Arming of the System

The "arming" of the system on the launch pad is split into three separate actions. The first is the arming of the rocket by pulling the arming pin. From this point on, the recovery system could be deployed. The second is the opening of the nitrogen bottles and the manual fill valve, allowing N<sub>2</sub> and N<sub>2</sub>O flow to be controlled via the electrically actuated valves. The third is the connection of the ignitor cable to the ignition box and the turning of the ignition key switch. Each action moves the personnel further away from the rocket, with the ignition box being placed 15 m from the rocket.

## 4.2 Abort Scenarios

The launch sequence can be aborted at any time before lift-off. An abort is conducted in the logical inverse way of arming the system. In the first step, the rocket is depressurised via its vent valve, if possible. After this, personnel approaches the ignition box to disconnect the ignitor. Next, the gas bottles are closed, and the fill lines are manually depressurised. Then, the rocket is disarmed by loosening the arming screws. Lastly, the rocket is vented via its manual relive valve if the electronically actuated venting earlier failed.

## 4.3 Thrust Curves

Figure 4.1 shows the measured thrust curves of all hot-fire tests. For the flight simulations, the thrust curve of HF 3.1 was used, as it is the lower limit on the initial thrust and therefore the lower limit concerning the off-the-rail velocity.

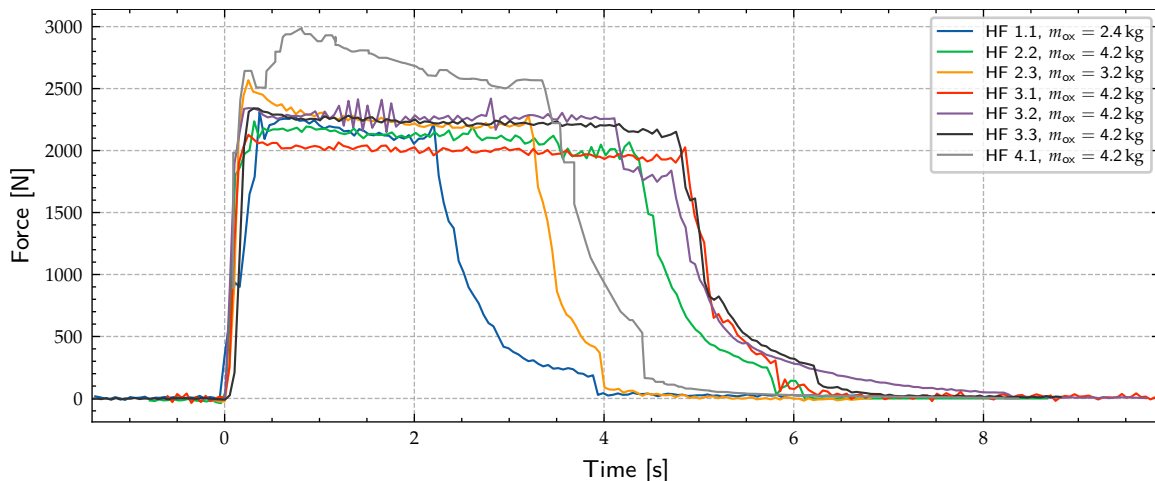


Figure 4.1: Thrust curves of all hot-fire tests. Note that their different burn duration is mainly due to different amounts of oxidizer used in the test. As can be seen, the thrust is mostly constant and of the same order for all but the last test.

## 4.4 Flight Simulation

Figure 4.2 shows the flight trajectory simulated with RocketPy for HALCYON. As already denoted in Table 4.1, the time until apogee is about 30 s, while the whole flight takes about 3.5 min. The off-the-rail velocity assuming the lowest thrust curve (HF 3.1) is 36 m/s, surpassing the 30 m/s required by EuRoC.

Table 4.2 shows the effect of different side wind velocities on the flight parameters. Notable is a slight decrease in apogee and an increase in drift distance (distance between the launch rail and the point of landing). The rocket remains within the limits for a stable flight of 1.5 to 6 body calibre. The calculations were done with OpenRocket as it includes the shift of the centre of pressure at speeds higher than 165 m/s.

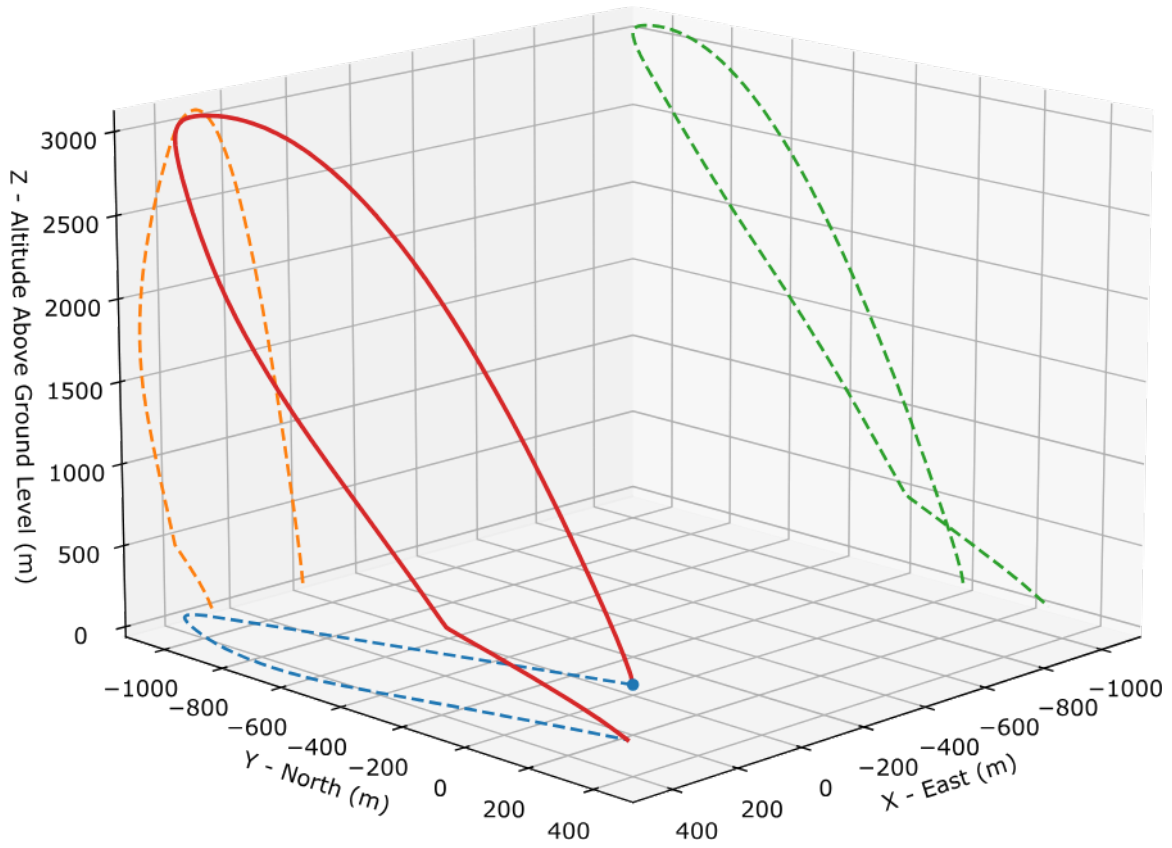


Figure 4.2: 3D Flight trajectory with RocketPy.

Table 4.2: OpenRocket simulation parameters for different side winds.

Side Wind [m/s]	Apogee [m]	$v_{max}$ [m/s]	$a_{max}$ [m/s <sup>2</sup> ]	Stability off Rail [calibers]	max. Stability [calibers]	max. Drift Distance [m]
0	3234	264	57.3	4.2	5.5	866
2	3195	264	57.2	3.5	5.5	1009
4	3145	264	57.2	2.7	5.5	1171
6	3085	264	57.2	2.5	5.5	1307
8	3015	263	57.2	2.1	5.5	1512

## 5 Conclusions and Outlook

With project HALCYON, we were able to achieve several things, first and foremost the safe landing of a rocket at the test flight in August, ready to fly again. This was a major step for us as ASTG, as in our history of two prior rocket launches, only ballistic landings with irreparable damage to the flight vehicle can be noted. Of course, a lot of lessons were learned in those previous projects, AVES and AVES II, and those contributed to the success of the HALCYON test flight. For our future projects, it can also only highlight the importance of planning for a test launch, and planning for multiple possible locations for that test. Like last year, we were set on conducting the flight here in Austria, at proving grounds of the Austrian army. But like last year, this proved to be difficult and in the end even impossible, as the necessary permits were never given out of safety concerns. Even when trying to clear up those safety concerns in a productive dialogue, we were only met with negative responses or no responses at all. Close to being out of time, it was a scramble to find an alternative testing site, which in the end was luckily possible at a model rocket launch weekend in Manching, Germany. While we were fortunate with the timing of this event, as it was on exactly the same day that we planned for anyways, it should not be left to luck in future projects. Even when people ensure with certainty that a test launch will be possible somewhere, alternatives should still be considered if that plan fails.

A second major achievement is the development of the pressurized hybrid propulsion system. At the beginning of the project we knew that plenty of work was cut out for us by making the decision of switching from the refined rocket candy boosters of AVES II to a new system. After finishing the design phase, there were already the first hurdles when it came to acquiring the many different parts we needed. Trying to plan for the lead times of COTS components and machined parts from our partners, there still proved to be unforeseen delays and so the first hot-fire tests had to be postponed. Shortening the schedule in this way brought a bigger workload for everyone involved during the integration of the complete system, and many days (and some long nights) had to be spent to get the rocket and the GSE to behave as intended. During this time, the team morale was hard to keep from dipping too low. But in the end, we managed to overcome the issues, which was awarded by several impressive test firings of the hybrid motor, and ultimately the successful launch. Over the coming weeks there still remain a few problems to solve, as some combustion instabilities were still present, and the remote disconnect of the umbilicals was not finished in time to be tested at the launch.

Also noteworthy this year is the reliability of the telemetry system. As learned in the previous two years, a dependable wireless connection with the rocket is difficult to achieve, and thus, work on the telemetry hard- and software started as early as possible. In doing so, the remote communication could undergo a lot of testing prior to the integration with other systems, and so it was almost always the system with the fewest problems. While this may seem obvious, it should still be a lesson for future projects that everything that has not been tested will not work when you want it to.

The last thing, and another takeaway from the test flight, is the difficulty of getting the recovery system fully working. It proved to be very hard, as it took us countless ground tests and a full rocket launch, and it still was not completely successful. For HALCYON, we will attempt our best to fix the issue of the main parachute being deployed together with the drogue, and for future projects, the importance of recovery system testing under real conditions cannot be overstated.



# List of Figures

1.1	Overview of the Team Demographics . . . . .	7
1.2	Team Organisational Structure . . . . .	8
2.1	Overview of the Launch Vehicle . . . . .	11
2.2	Propulsion Stack . . . . .	12
2.3	Fluid system of the Rocket. . . . .	13
2.4	Upper Fluid System . . . . .	14
2.5	Valvebay Section . . . . .	15
2.6	Nozzle section . . . . .	16
2.7	Bulkhead section . . . . .	16
2.8	Swirl Injector . . . . .	17
2.9	Mixing Device model. . . . .	17
2.10	Screw Ignitor . . . . .	18
2.11	Vertical Hot-Fire Test Setup . . . . .	19
2.12	Overview of Air Frame . . . . .	20
2.13	Visualized Results of CFD Simulation . . . . .	21
2.14	Tail Camera Assembly . . . . .	21
2.15	View of Fins . . . . .	22
2.16	Sectional View of Nose Cone . . . . .	22
2.17	Payload Retainer FEA . . . . .	23
2.18	Radax Joint . . . . .	23
2.19	Oxidizer Tank Overview . . . . .	24
2.20	Top of Oxidizer Tank . . . . .	25
2.21	Thrust Structure . . . . .	26
2.22	Railbutton Assembly . . . . .	26
2.23	Sectional View of Recovery System . . . . .	27
2.24	Exploded View of First Deployment . . . . .	27
2.25	Assembled First Deployment . . . . .	28
2.26	Assembled Pressure Plate with First Deployment . . . . .	28
2.27	Detailed Views of Second Deployment System . . . . .	29
2.28	Assembled Recovery Groundplate . . . . .	30
2.29	Drogue Parachute . . . . .	31
2.30	Main Parachute . . . . .	31
2.31	Main Parachute Bag . . . . .	32
2.32	Thimble, Rope Protection, and Rotatable Carabiner . . . . .	32
2.33	Line Management after First Deployment . . . . .	33
2.34	Line Management after Second Deployment . . . . .	34
2.35	Overview of Recovery Electronics . . . . .	35
2.36	Fully equipped CANary . . . . .	36
2.37	Rocket Power System . . . . .	37
2.38	Electronics Mount . . . . .	37
2.39	Mainboard and Backplane . . . . .	38
2.40	Rocket FC State Diagram . . . . .	39
2.41	Automatic State Detection . . . . .	40
2.42	Overview of Telemetry System . . . . .	41
2.43	Mission Control Visualization . . . . .	42

2.44	Main Board	43
2.45	FSK Board	43
2.46	LoRa Board	43
2.47	GS Backplane	43
2.48	Model of Antenna Bay	44
2.49	Patch Antenna Ring	44
2.50	CAD of Cubesat Colibri	45
2.51	Foto of Cubesat PATHOA	45
3.1	Fluid System Schematic of the Filling Station	47
3.2	Diagram of Ignition Electronics	48
3.3	State Diagram of the Filling Station	49
3.4	Umbilical Arm with Quick Disconnects	50
3.5	Schematic of the Cooling Cycle	51
3.6	Mission Control Setup without Antennas	52
4.1	Combined Thrust Curves	55
4.2	3D Flight trajectory with RocketPy	56
B.1	Overview of Recovery Electronics	71
B.2	Tanking Procedure	245
B.3	Tanking Pressure Hysteresis	246

# List of Tables

2.1	Main rocket engine characteristics. . . . .	12
2.2	Summary of HALCYON hot-fire results. . . . .	19
2.3	Properties of airframe winded tubes. . . . .	20
4.1	Tabulated Concept of Operations . . . . .	53
4.2	glsopenrocket Simulation Parameters . . . . .	56
A.1	System Data - Outer Dimensions and Mass Distribution . . . . .	67
A.2	System Data - Flight Data . . . . .	67
A.3	System Data - Aerostructure . . . . .	67
A.4	System Data - Propulsion . . . . .	68
A.5	System Data - Recovery . . . . .	68
A.6	System Data - Flight Computer . . . . .	68
A.7	System Data - Telemetry . . . . .	69
A.8	System Data - Payload . . . . .	69
B.1	Tabulated Testing List . . . . .	304

# List of Acronyms

<b>ABS</b>	Acrylnitril-Butadien-Styrol
<b>ADC</b>	Analog-to-Digital Converter
<b>ALL</b>	All modules of the project HALCYON
<b>API</b>	Application Programming Interface
<b>ASA</b>	Acrylnitril-Styrol-Acrylester
<b>AST</b>	Aerostructure module
<b>ASTG</b>	Aerospace Team Graz
<b>ATP</b>	ASTG Transport Protocol
<b>AVI-S</b>	Avionics Section
<b>AW</b>	Aluminium Wrought
<b>BMK</b>	Austrian Federal Ministry for Climate Action, Environment, Energy, Mobility, Innovation and Technology
<b>CAN</b>	Controller Area Network
<b>CATS</b>	Control And Telemetry Systems
<b>CeFRP</b>	Ceramic Fibre Reinforced Polymer
<b>CFD</b>	Computational Fluid Dynamics
<b>CFRP</b>	Carbon Fibre Reinforced Polymer
<b>CoG</b>	Center of Gravity
<b>COPV</b>	Composite Overwrapped Pressure Vessel
<b>COTS</b>	Commercial Off The Shelf
<b>CT</b>	Coupling Tube
<b>DC</b>	Direct Current
<b>DMA</b>	Direct Memory Access
<b>EMI</b>	Electro Magnetic Interference
<b>EN</b>	European Norm
<b>ESA</b>	European Space Agency
<b>EVA</b>	Ethylen Vinyl Acetate
<b>EuRoC</b>	European Rocketry Challenge
<b>FC</b>	Flight Computer
<b>FEA</b>	Finite Element Analysis
<b>FEM</b>	Front End Module
<b>FLI</b>	Flightcomputer module
<b>FS</b>	Filling Station
<b>FSK</b>	Frequency-Shift Keying
<b>GFRP</b>	Glass Fibre Reinforced Polymer
<b>GNSS</b>	Global Navigation Satellite System
<b>GPS</b>	Global Positioning System
<b>GS</b>	Ground Station
<b>GSE</b>	Ground Support Equipment
<b>HTTP</b>	Hypertext Transfer Protocol
<b>IC</b>	Integrated Circuit
<b>ISM</b>	wireless band for Industrial, Scientific, and Medical purposes
<b>IFT</b>	Institute of Manufacturing Engineering
<b>IIM</b>	Institute of Innovation and Industrial Management
<b>IMU</b>	Inertial Measurement Unit

**LAN** Local Area Network  
**LNA** Low Noise Amplifier  
**LED** Light-Emitting Diode  
**Li-Ion** Lithium-Ion  
**LiFePO<sub>4</sub>** Lithium Iron Phosphate  
**MC** Mission Control  
**MCU** Micro Controller Unit  
**NC** Nitrocellulose  
**NC-S** Nose Cone Section  
**OT-S** Oxidizer Tank Section  
**PA** Power Amplifier  
**PA 12** Polyamid 12/Nylon 12  
**PBO** Poly(p-phenylene-2,6-benzobisoxazole), Zylon<sup>®</sup>  
**PC** Personal Computer  
**PCB** Printed Circuit Board  
**PCIe** Peripheral Component Interconnect Express  
**PET** Polyethylene Terephthalate  
**PLA** Polylactic Acid  
**PRO** Propulsion module  
**PTFE** Polytetrafluoroethylene  
**PU** Polyurethane  
**PWM** Pulse Width Modulation  
**QD** Quick Disconnect  
**REC** Recovery module  
**REC-S** Recovery Section  
**RCD** Residual Current Device  
**RF** Radio Frequency  
**RTOS** Real-Time Operating System  
**SLS** Selective Laser Sintering  
**SRAD** Student Researched And Developed  
**T-S** Tail Section  
**TDD** Time-Division Duplexing  
**TEL** Telemetry module  
**TIG** Tungsten Inert Gas  
**TUG** Graz University of Technology  
**TPU** Thermoplastic polyurethane  
**UART** Universal Asynchronous Receiver Transmitter  
**USB** Universal Serial Bus  
**WLAN** Wireless Local Area Network (LAN)

# Glossary

- 3D-print** Additive manufacturing process. 17, 18, 21, 22, 25, 26, 28, 30, 38, 50
- 3M™ Scotch-Weld™ DP 490** Two-component epoxy resin-based construction adhesive. 22
- airframe** Mechanical structure of rocket. 3, 8, 11, 20, 37, 67
- Antenna Bay** Internal antenna with RF shielding against rest of rocket. 37, 44, 52
- AVES** ASTG rocket for the 2021 EuRoC, category S3. 7, 57
- AVES II** ASTG rocket for the 2022 EuRoC, category S3. 7, 57
- Backplane** PCB that serves as interconnection between slot-in PCBs. 36, 42, 43, 60
- Blackbox** Hardened data storage designed to survive ballistic impacts. 35
- CAN Bus** bus consisting of multiple devices using the CAN protocol. 36
- CANary** Control and data acquisition module connected via Controller Area Network (CAN) bus. 35, 36, 48, 50, 59
- cold-flow** Rocket engine test with oxidizer without ignition. 17, 18, 247
- CubeSat** Miniaturized satellite with form factor of 100 mm cube. 3, 9, 11, 22, 45, 69
- Demonstrator** Smaller self pressurized hybrid test engine. 7, 16, 18, 126
- HALCYON** ASTG rocket for the 2023 EuRoC, category H3. 3, 7–9, 12, 13, 18–21, 35, 38, 45, 53, 55, 57, 61, 62, 71, 126
- hot-fire** Rocket engine firing test. 12, 18, 19, 55, 57, 61, 126, 138, 247
- HTL** Polytechnical High School - German: "Höhere Technische Lehranstalt". 45
- Lay-Up** Process of moulding composite materials by layering the fibres. 20, 22
- Liquid CaSi** A solution of amyl-CaSi which is used as an ignition accelerator. 18
- LoRa** Radio communication technique. 41, 43, 44, 52, 60, 69
- Mission Control Box** Box that houses the telemetry components in the Mission Control. 39, 41–43, 52
- nose cone** Cone-shaped front part of the rocket. 3, 11, 21–23, 45
- OpenRocket** Rocket flight simulation software. 55, 56
- Radax** Radial-Axial, a type of airframe joint, describing the angled contact surface and force transfer. 20, 23–25
- RavenOS** Self-developed RTOS running on the main FC. 38
- RocketPy** Rocket flight simulation program based on python. 55, 56, 60
- RP2040** Microcontroller from Raspberry Pi. 43
- tail cone** Cone-shaped cover at the rear of the rocket. 11, 21
- test stand** Platform for tests. 18

## References

- [1] Mohammad Mahdi Heydari and Nooredin Ghadiri Massoom. "Experimental Study of the Swirling Oxidizer Flow in HTPB/N<sub>2</sub>O Hybrid Rocket Motor". In: *International Journal of Aerospace Engineering* 2017 (2017), Article ID 3174140, 10 pages. DOI: 10.1155/2017/3174140.
- [2] Colin D. Hill, Will Nelson, and Craig T. Johansen. "Evaluation of a Paraffin/Nitrous Oxide Hybrid Rocket Motor with a Passive Mixing Device". In: *Journal of Propulsion and Power* 38.6 (2022), November–December 2022. DOI: 10.2514/1.B38659.
- [3] D. Poynter. *The Parachute Manual: A Technical Treatise on Aerodynamic Decelerators*. The Parachute Manual: A Technical Treatise on Aerodynamic Decelerators Bd. 1. Para Pub., 1984. ISBN: 9780915516353. URL: <https://books.google.at/books?id=BKTuTXrXQu0C>.
- [4] Tobias Scheipel et al. "SmartOS: An OS Architecture for Sustainable Embedded Systems". In: *Tagungsband des FG-BS Frühjahrstreffens 2022* (Mar. 2022). DOI: 10.18420/fgbs2022f-01.



## Appendix A: System Data

Table A.1: System Data - Outer Dimensions and Mass Distribution

Total Length	3568 mm
Diameter	152.4 mm
Total Mass	32 kg
Mass Airframe Tail Section	1119 g
Mass Oxidizer Tank	3223 g
Mass Airframe Avionics Section	1459 g
Mass Avionics Stack	1814 g
Mass Airframe Recovery Section	1430 g
Mass Recovery Subsystem	4350 g
Mass Airframe Nose Cone Section	1570 g
Mass Payload	3990 g
Mass COTS CATS incl. Mounting	1590 g

Table A.2: System Data - Flight Data

Target Apogee	3000 m
Velocity off Rod	37 m/s
Max. Velocity	264 m/s
Max. Acceleration	57.3 m/s <sup>2</sup>
Time to Apogee	26 s
Total Flight Time	218 s

Table A.3: System Data - Aerostructure

Drag Coefficient	0.26 to 0.37
Center of Gravity (reference: tip)	1204 mm
Moment of Inertia	172.44 kg m <sup>2</sup>
Fin Geometry	Trapezoidal

Table A.4: System Data - Propulsion

Engine	SRAD Hybrid
Fuel	Paraffin with Additives
Fuel Mass	1150 g
Oxidizer	Nitrous Oxide (N <sub>2</sub> O)
Oxidizer Mass	4200 g
Pressurizing Gas	Nitrogen (N <sub>2</sub> )
Total Impulse	11 000 N s
Max. Thrust	2500 N
Burn Time	5 s
Max. expected Chamber Pressure	40 bar
Nominal Chamber Pressure	35 bar
Dry Mass	9800 g
Length	1523 mm
Ignition Type	Pyro

Table A.5: System Data - Recovery

First Deployment Event	Apogee (3000 m)
Main Deployment Event	450 m AGL
Descent Velocity Drogue Parachute	38.87 m/s
Descent Velocity Main Parachute	2.38 m/s
Drag Coefficient Drogue Parachute	3
Drag Coefficient Main Parachute	10.5
Diameter Drogue Parachute	0.36 m
Diameter Main Parachute	3.2 m
Reference Area Drogue Parachute	0.1225 m <sup>2</sup>
Reference Area Main Parachute	7.7 m <sup>2</sup>
Opening Shock Drogue	1418 N
Opening Shock Main	3807 N

Table A.6: System Data - Flight Computer

Standby Time with Umbilical Connection	> 24 h
Standby Time without Umbilical Connection	> 4 h
Barometer Sampling Frequency	50 Hz
Processor Frequency	480 MHz
Redundancy Data Storage	2
Qty. Sensors (complete Rocket, without COTS)	49
Qty. PCBs (complete Rocket, without COTS)	16
Qty. Cameras (excluding Payload)	4

Table A.7: System Data - Telemetry

#1 System Type	LoRa (Rocket)
#1 Frequency Range	2435 to 2437 MHz
#1 Bandwidth	1.6 MHz
#1 RF Power	1 W
#1 Data Uplink	Configuration Parameters
#1 Data Downlink	Flight Data
#1 Range	> 16 km
#2 System Type	FSK (Rocket)
#2 Frequency Range	430 to 440 MHz
#2 Bandwidth	100 kHz
#2 RF Power	6.5 W
#2 Data Uplink	Configuration Parameters
#2 Data Downlink	Flight Data
#2 Range	> 16 km
#3 System Type	LoRa (Filling Station)
#3 Frequency Range	2400 to 2450 MHz
#3 Bandwidth	1.6 MHz
#3 RF Power	1 W
#3 Data Uplink	Configuration Parameters
#3 Data Downlink	FS data
#3 Range	> 16 km

Table A.8: System Data - Payload

Form Factor	CubeSat 100 × 100 × 113.5 mm
Mass per CubeSat	1300 to 1330 g
Qty. Payloads	3

